Energy Density Functional Studies of Exotic Nuclear Structure

Dario Vretenar
University of Zagreb

Energy Density Functionals

Consistent microscopic framework for a unified description of bulk properties, excitations and reactions!

Ab initio:
Quantum Monte Carlo,
No-core Shell Model,
Coupled-Cluster, ...

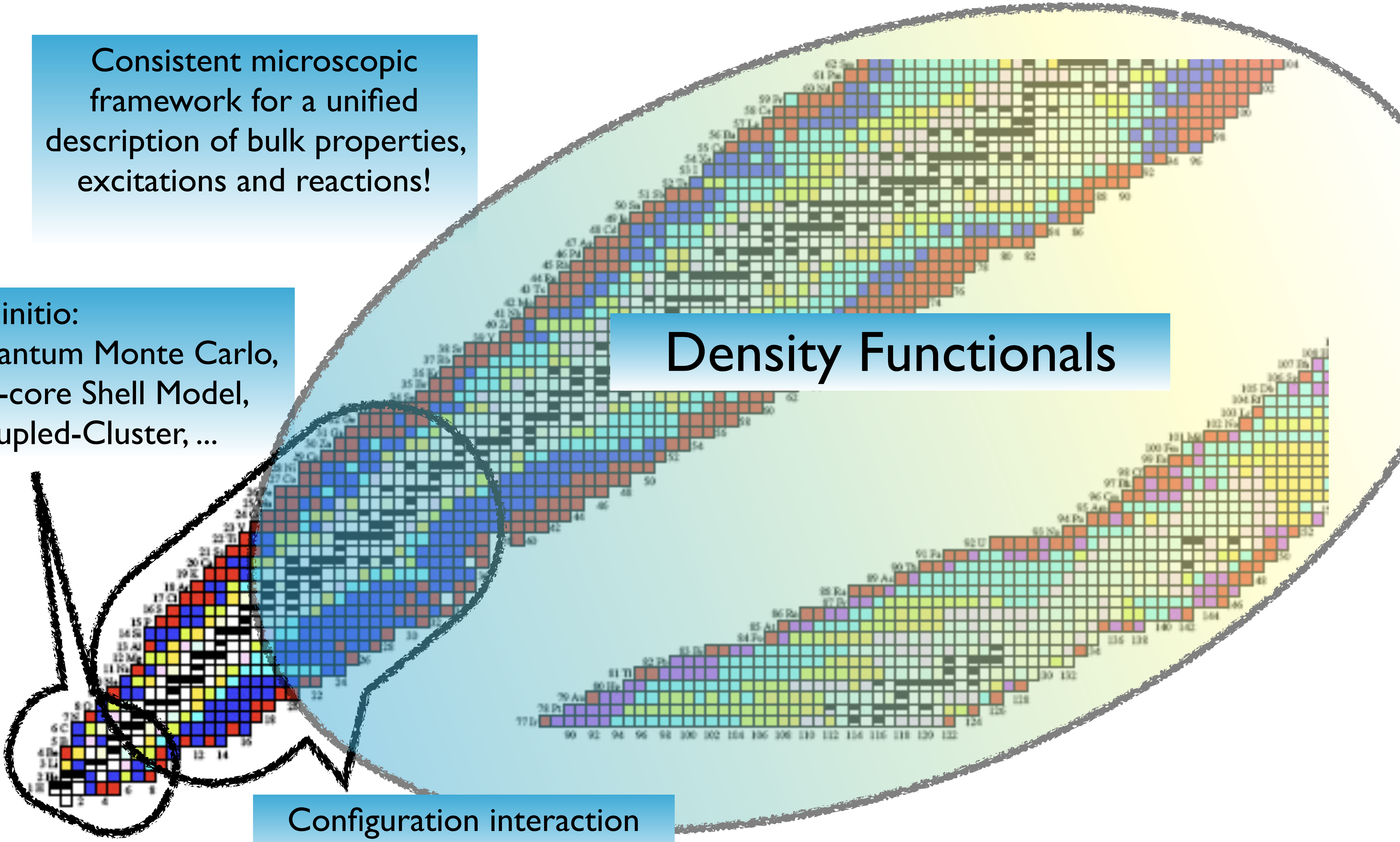

Density Functionals

Configuration interaction
(Interacting Shell-Model)

Energy Density Functionals

✔ the nuclear many-body problem is effectively mapped onto a ***one-body problem*** without explicitly involving inter-nucleon interactions!

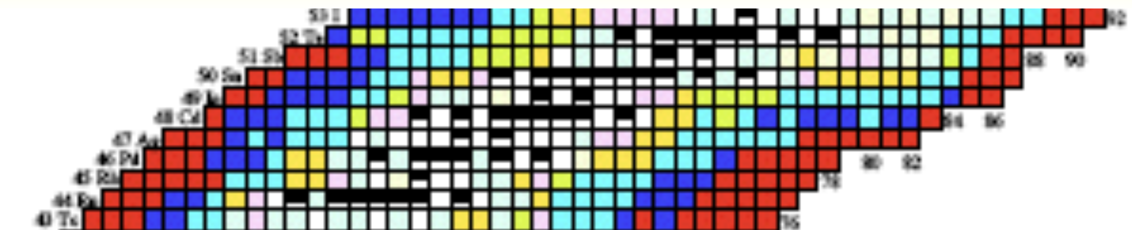

✔ the exact density functional is approximated with ***powers and gradients of ground-state densities and currents.***

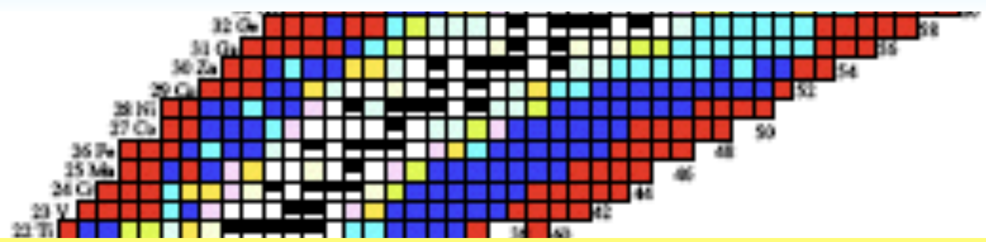

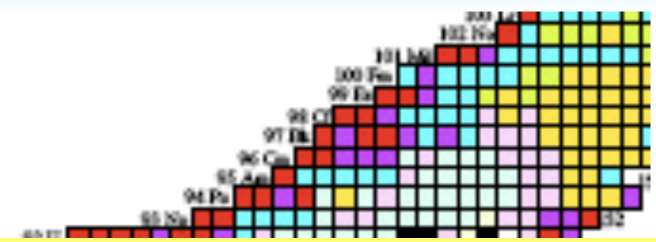

✔ ***universal density functionals*** can be applied to all nuclei throughout the chart of nuclides.

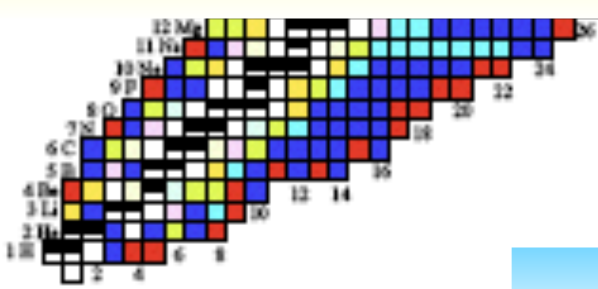

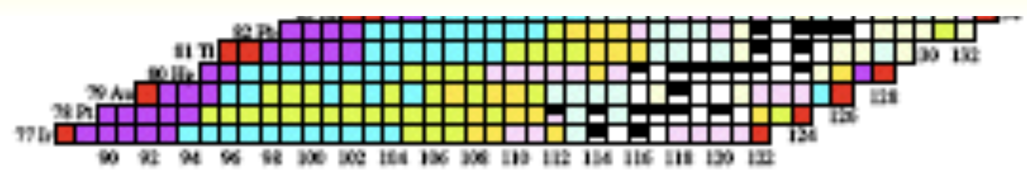

Important for extrapolations to regions far from stability!

✔ an intuitive interpretation of mean-field results in terms of ***intrinsic shapes*** and ***single-particle states***

✔ the ***full model space*** of occupied states can be used; no distinction between core and valence nucleons, ***no need for effective charges!***

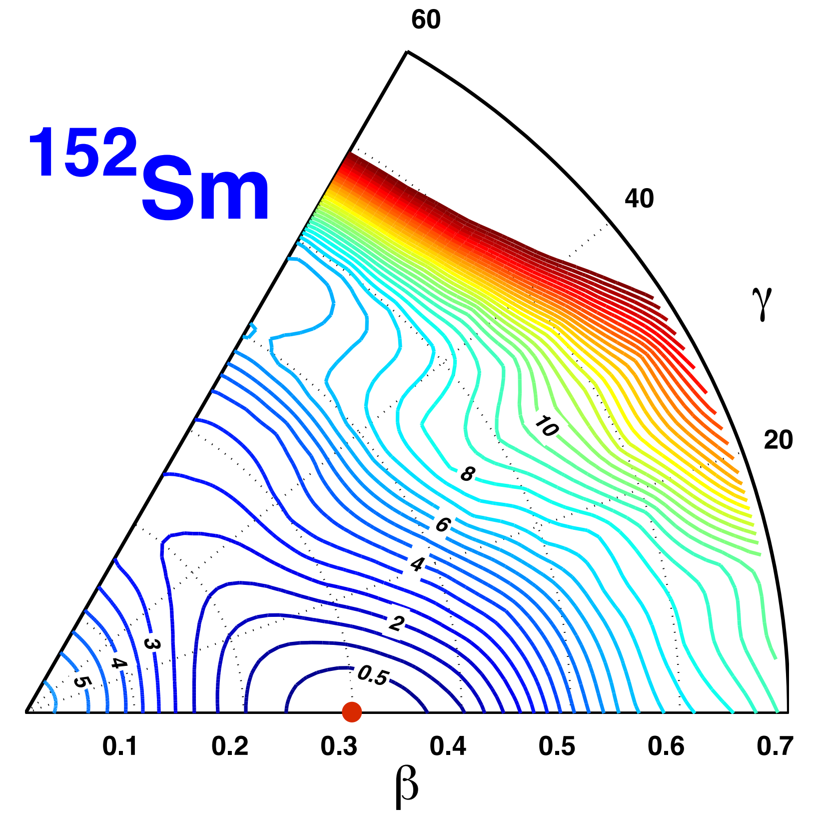

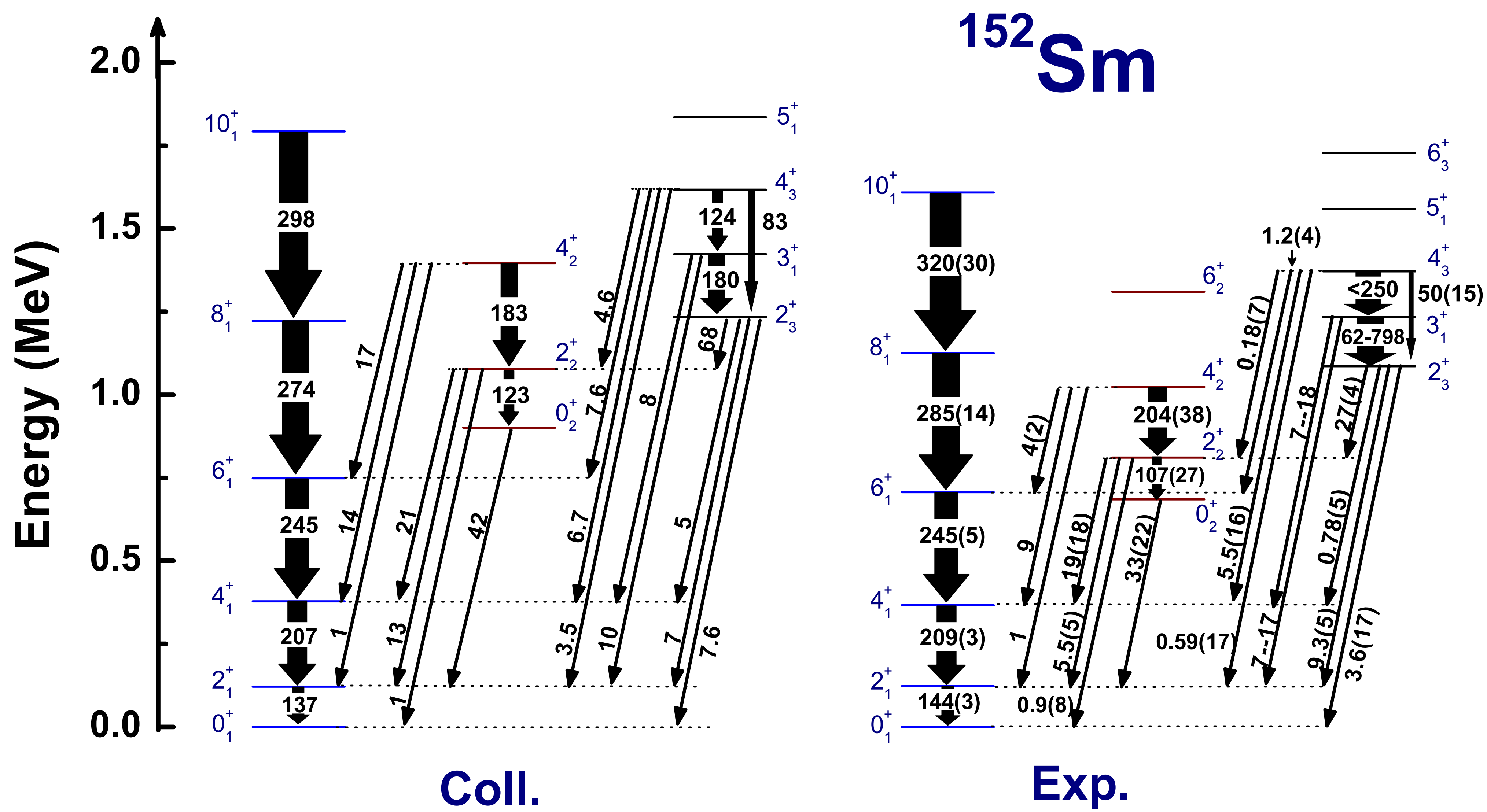

Nuclear Many-Body Correlations

short-range
(hard repulsive core of the NN-interaction)

long-range
nuclear resonance modes
(giant resonances)

collective correlations
large-amplitude soft modes:
(center of mass motion, rotation, low-energy quadrupole vibrations)

...vary smoothly with nucleon number!
Can be included implicitly in an effective Energy Density Functional.

...sensitive to shell-effects and strong variations with nucleon number!
Cannot be included in a simple EDF framework.

Collective correlations

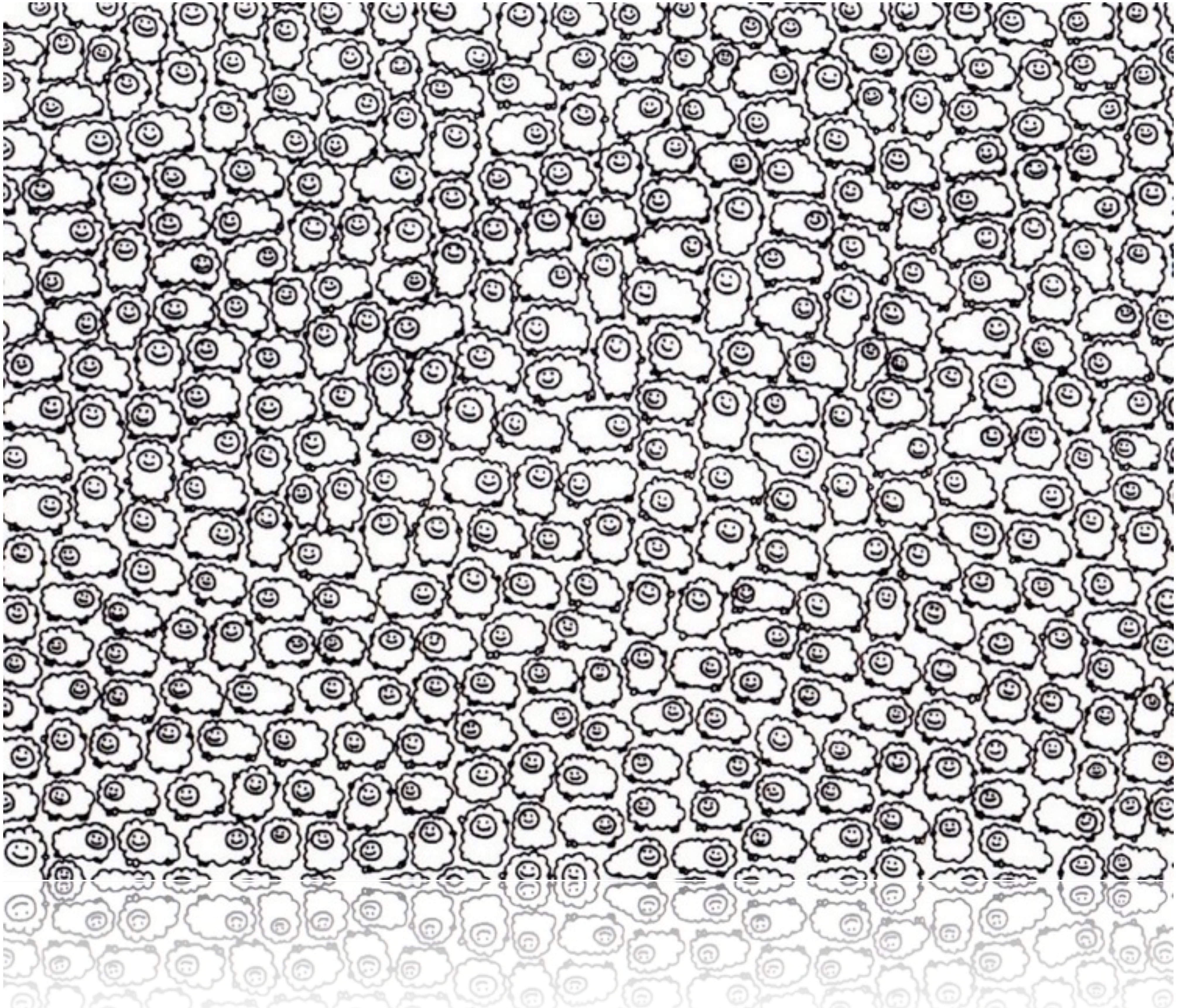

Shape evolution and triaxiality in germanium isotopes

T. Nikšić, P. Marević, and D. Vretenar

PHYSICAL REVIEW C **89**, 044325 (2014)

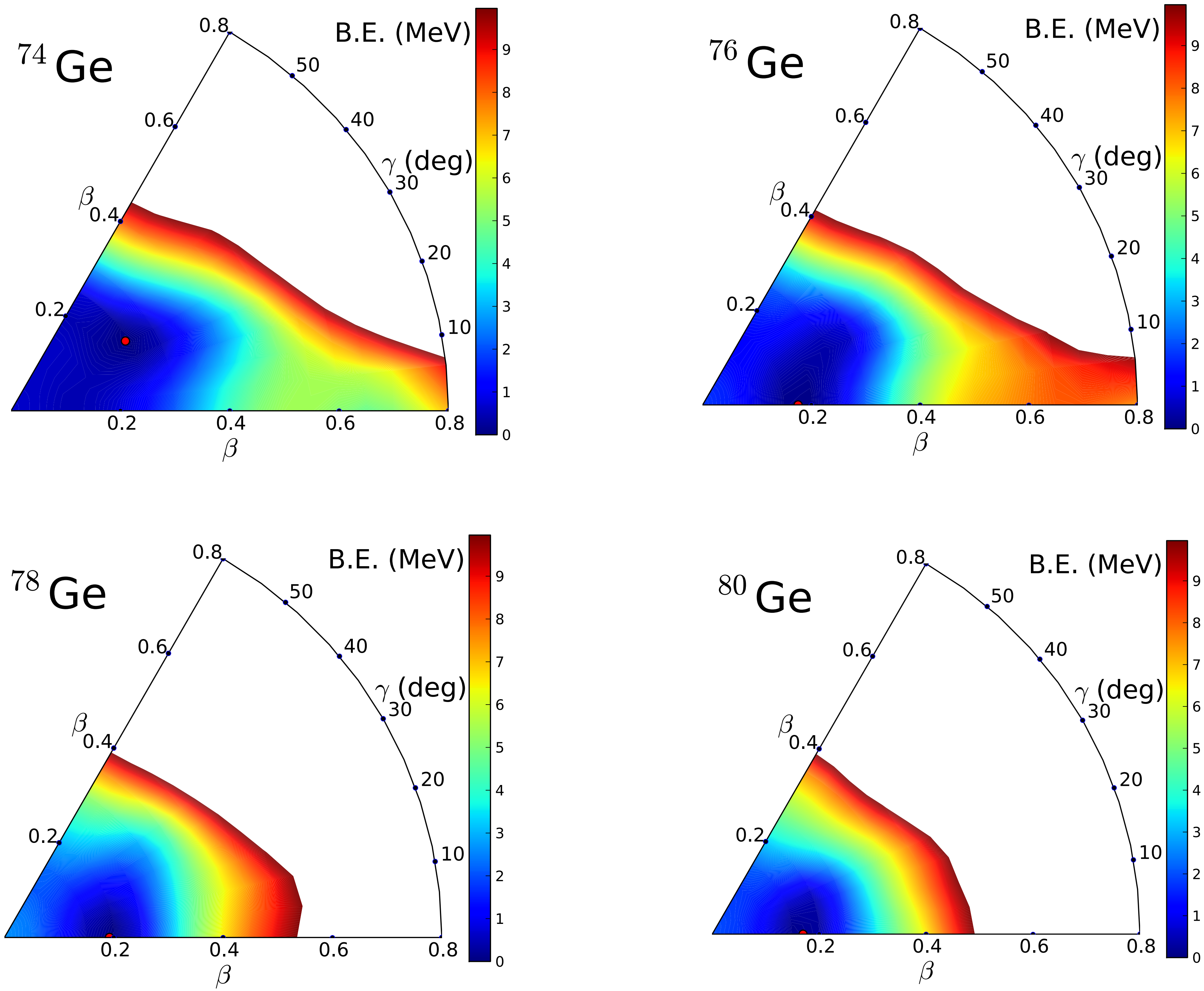

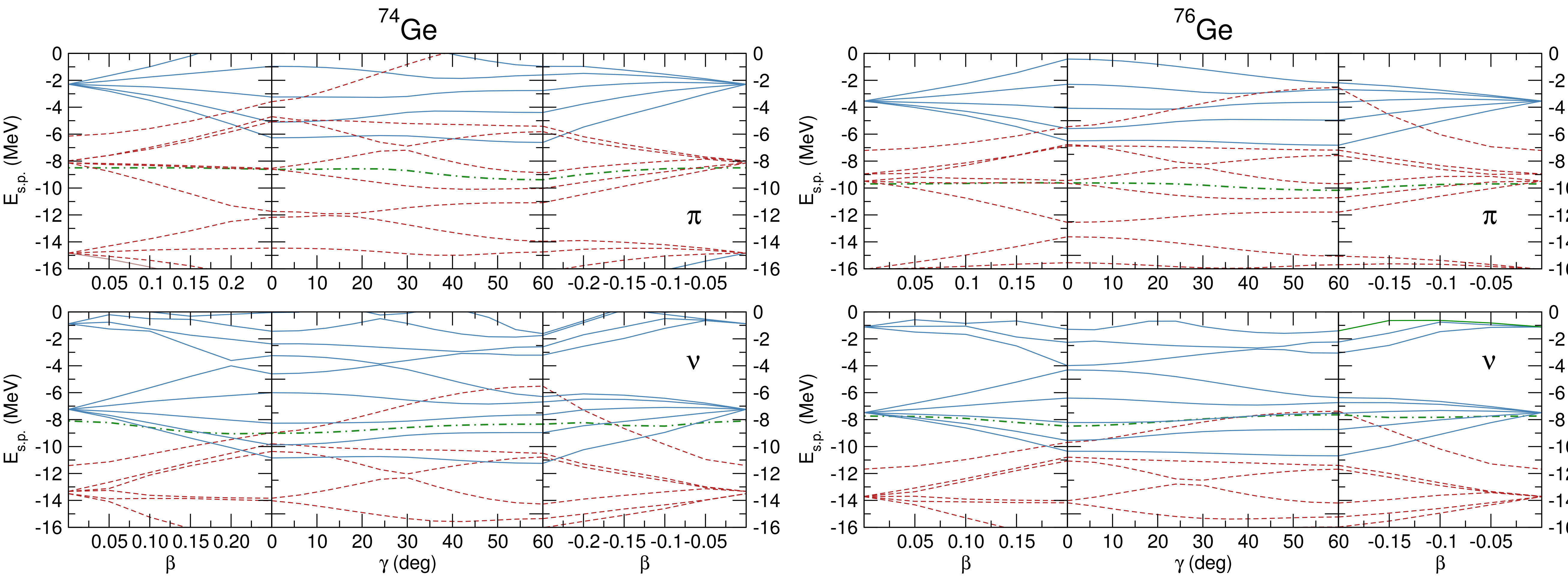

74Ge
76Ge
Es.p. (MeV)
π
ν
β
γ (deg)

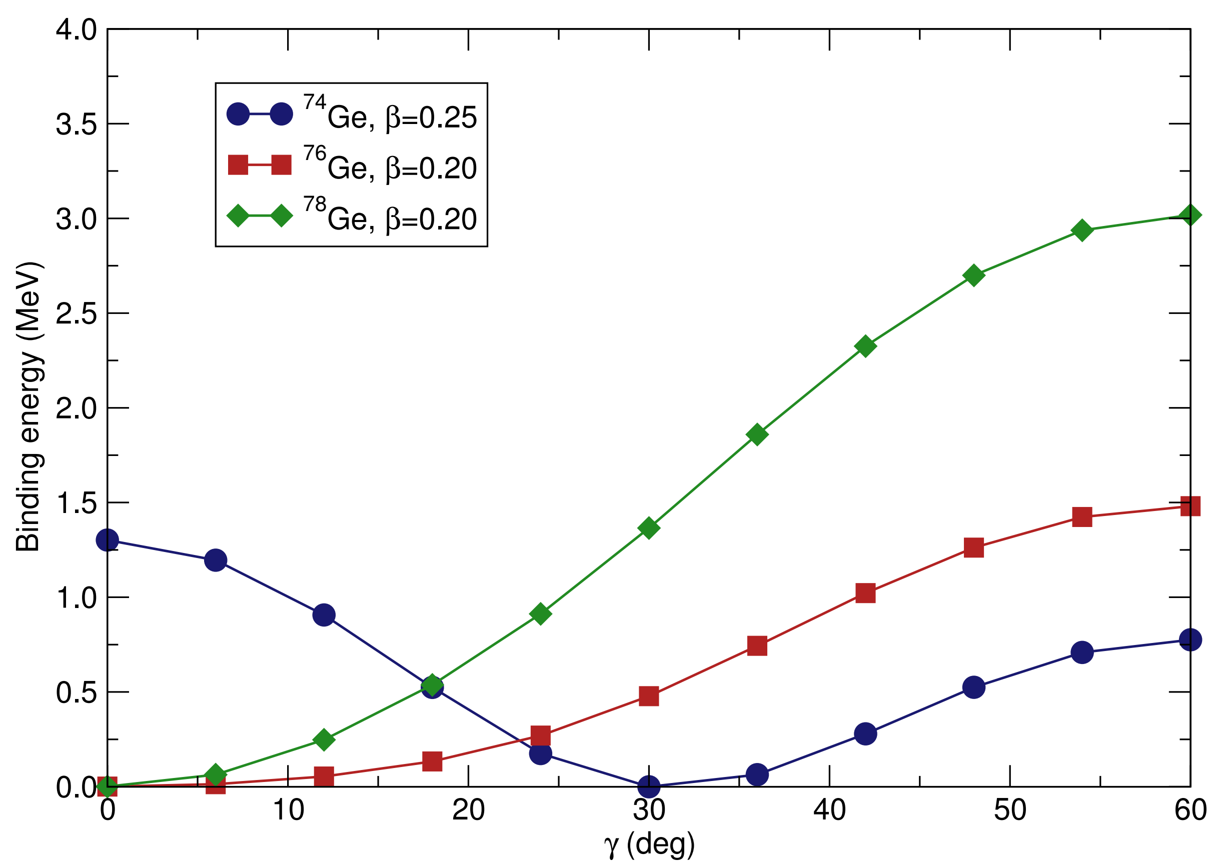

74Ge, β=0.25
76Ge, β=0.20
78Ge, β=0.20
Binding energy (MeV)
γ (deg)

Quadrupole collective Hamiltonian based on the functional DD-PC1

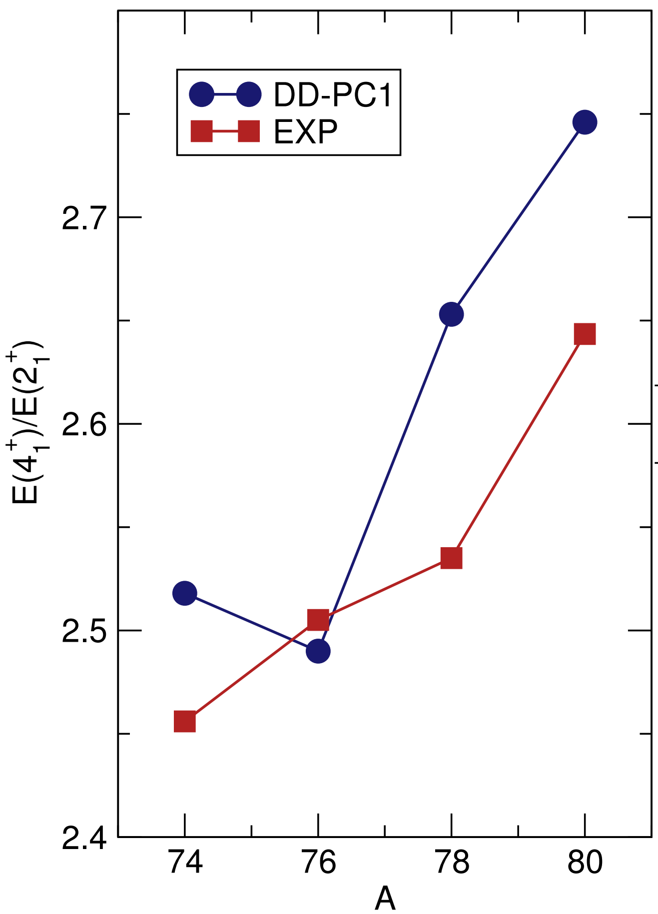

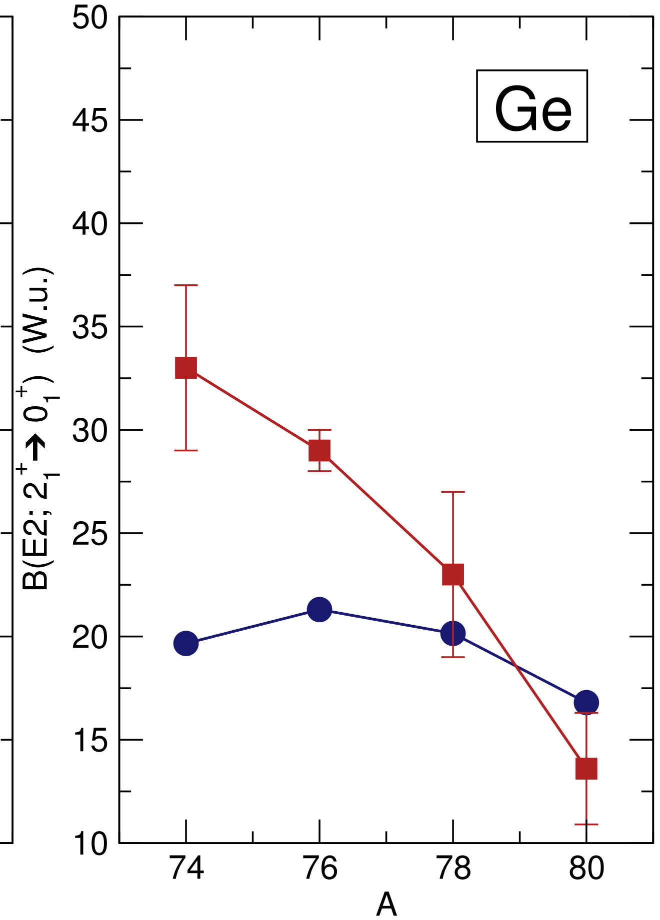

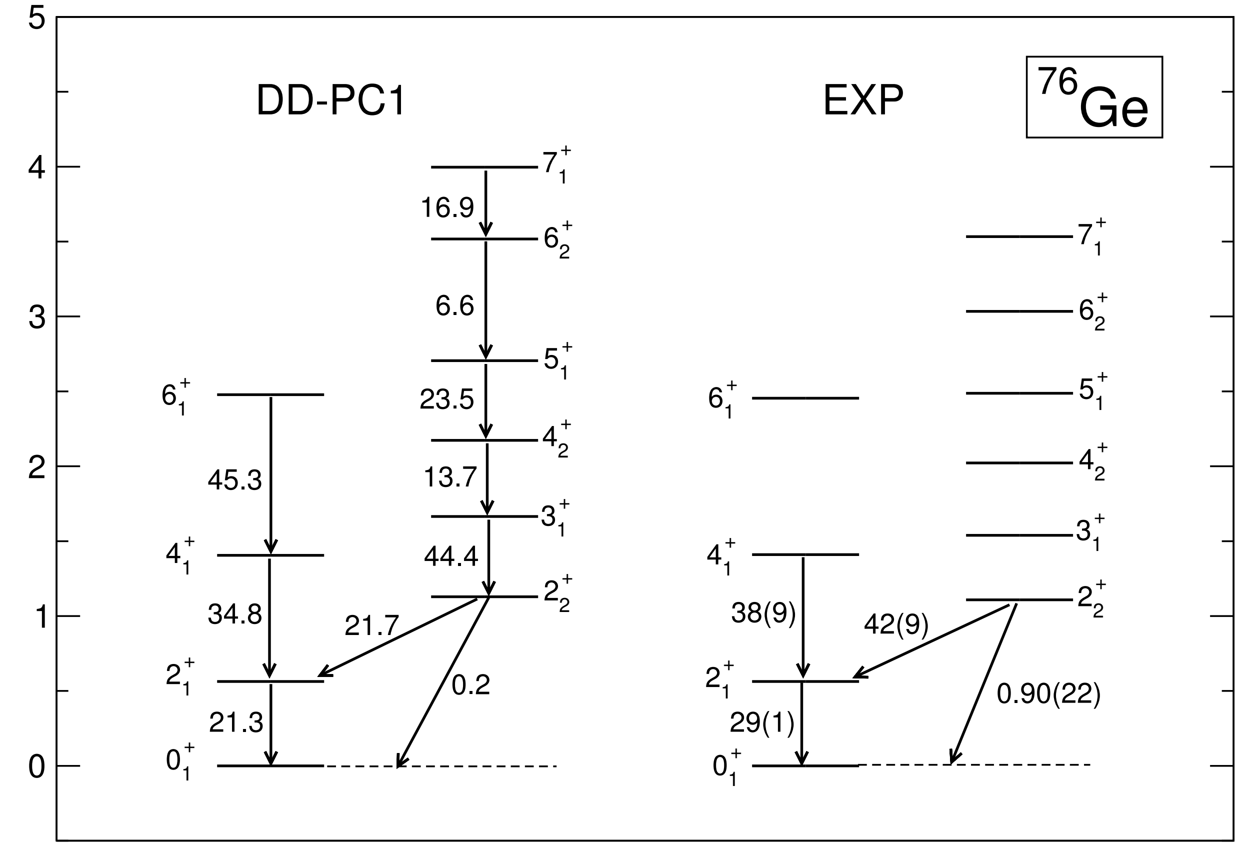

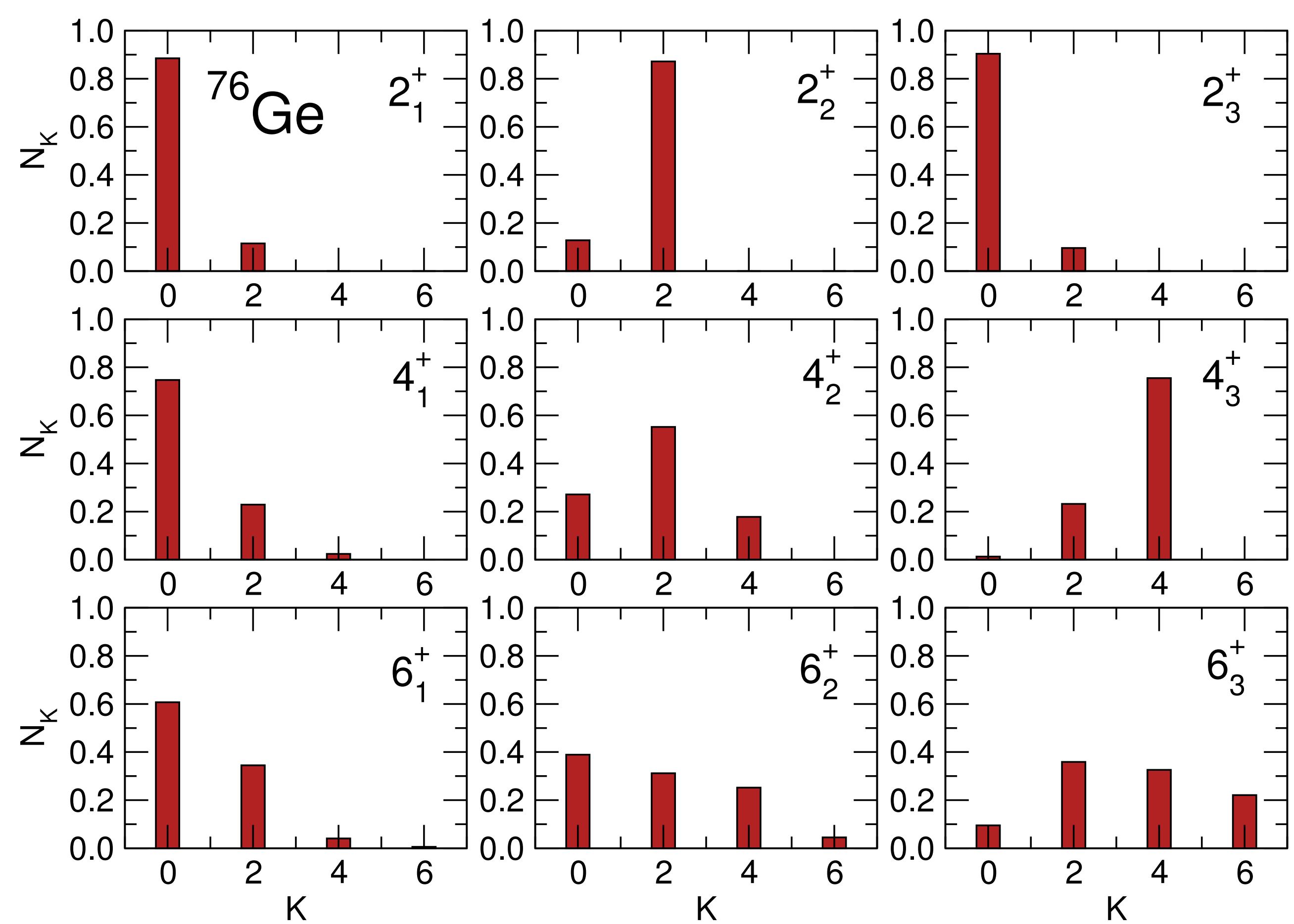

Distribution of K components (projection of the angular momentum on the body-fixed symmetry axis) in the collective wave functions of the nucleus ^{76}Ge.

The level of K-mixing is reflected in the staggering in energy between odd- and even-spin states in the γ band:

$$S(J) = \frac{E[J_\gamma^+] - 2E[(J-1)_\gamma^+] + E[(J-2)_\gamma^+]}{E[2_1^+]}$$

Deformed γ-soft potential ⇒ S(J) oscillates between negative values for even-spin states and positive values for odd-spin states.

γ-rigid triaxial potential ⇒ S(J) oscillates between positive values for even-spin states and negative values for odd-spin states.

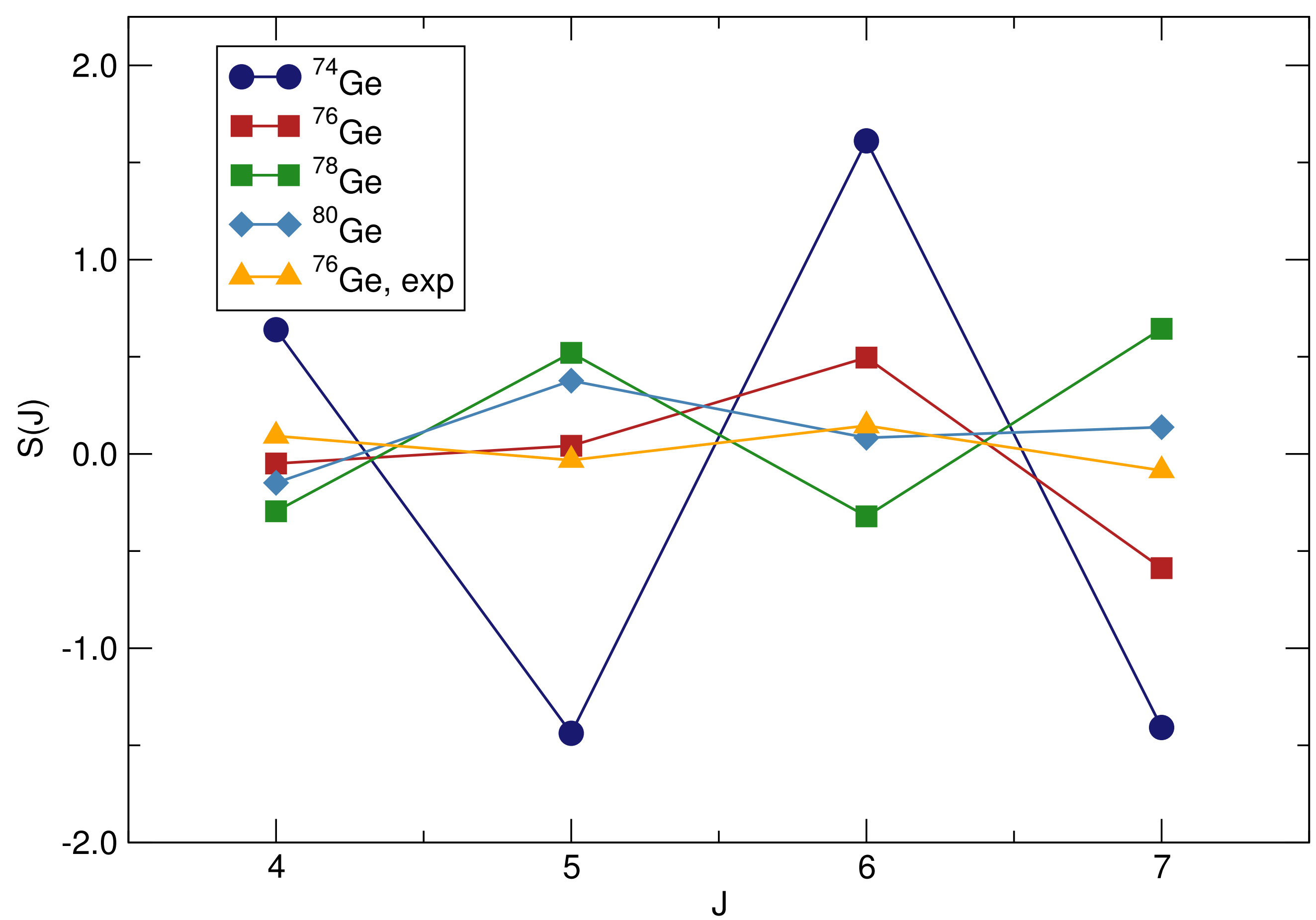

The mean-field potential of ^{76}Ge is γ soft. The inclusion of collective correlations (symmetry restoration and quantum fluctuations) drives the nucleus toward triaxiality, but they are not strong enough to stabilize a $\gamma \approx 30^\circ$ triaxial shape.

Octupole shape-phase transitions in light actinide and rare-earth nuclei

NOMURA, VRETENAR, NIKŠIĆ, AND LU PHYSICAL REVIEW C **89**, 024312 (2014)

Axially symmetric deformation energy surfaces of $^{222-232}Th$ in the (β_2,β_3) plane:

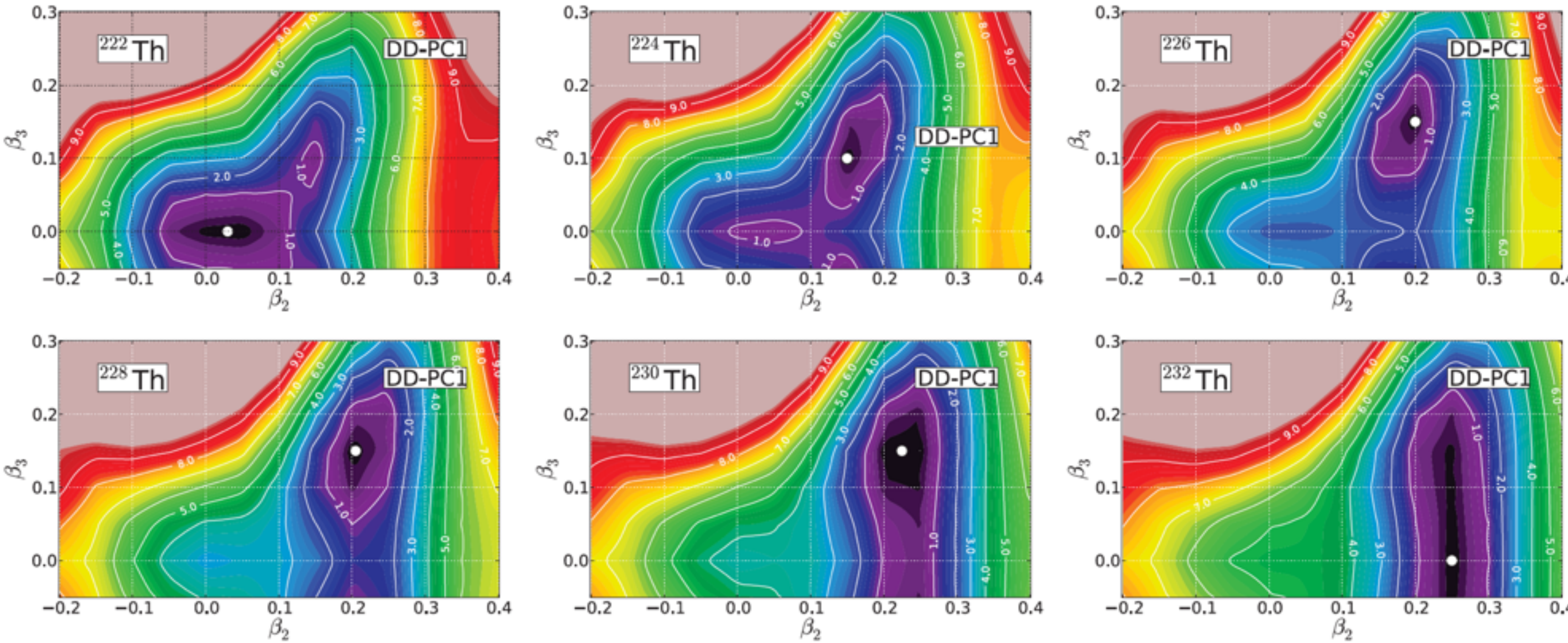

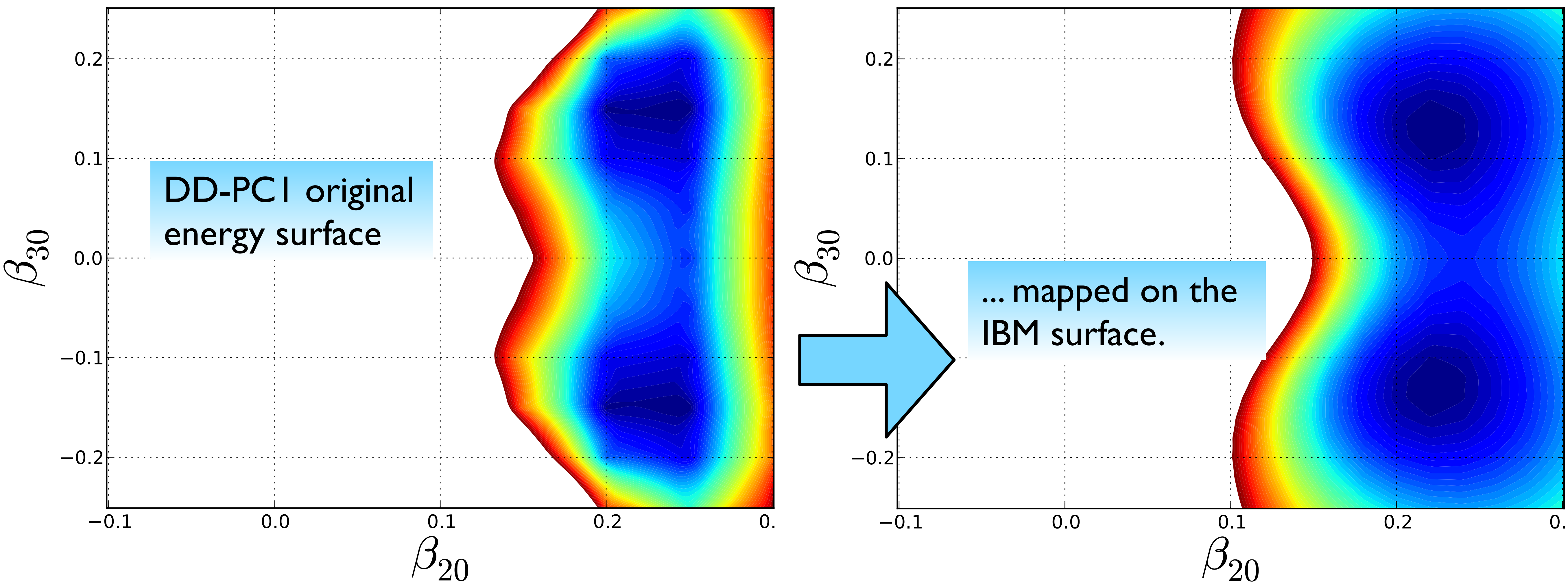

Mapping the microscopic PES on the expectation value of the IBM Hamiltonian in the *sdf*-boson condensate state:

$$\hat{H} = \epsilon_d \hat{n}_d + \epsilon_f \hat{n}_f + \kappa_2 \hat{Q} \cdot \hat{Q} + \alpha \hat{L}_d \cdot \hat{L}_d + \kappa_3 : \hat{V}_3^\dagger \cdot \hat{V}_3 :$$

$$|\phi\rangle = \frac{1}{\sqrt{N!}} (\lambda^\dagger)^N |-\rangle \qquad \lambda^\dagger = s^\dagger + \beta_2 d_0^\dagger + \beta_3 f_0^\dagger$$

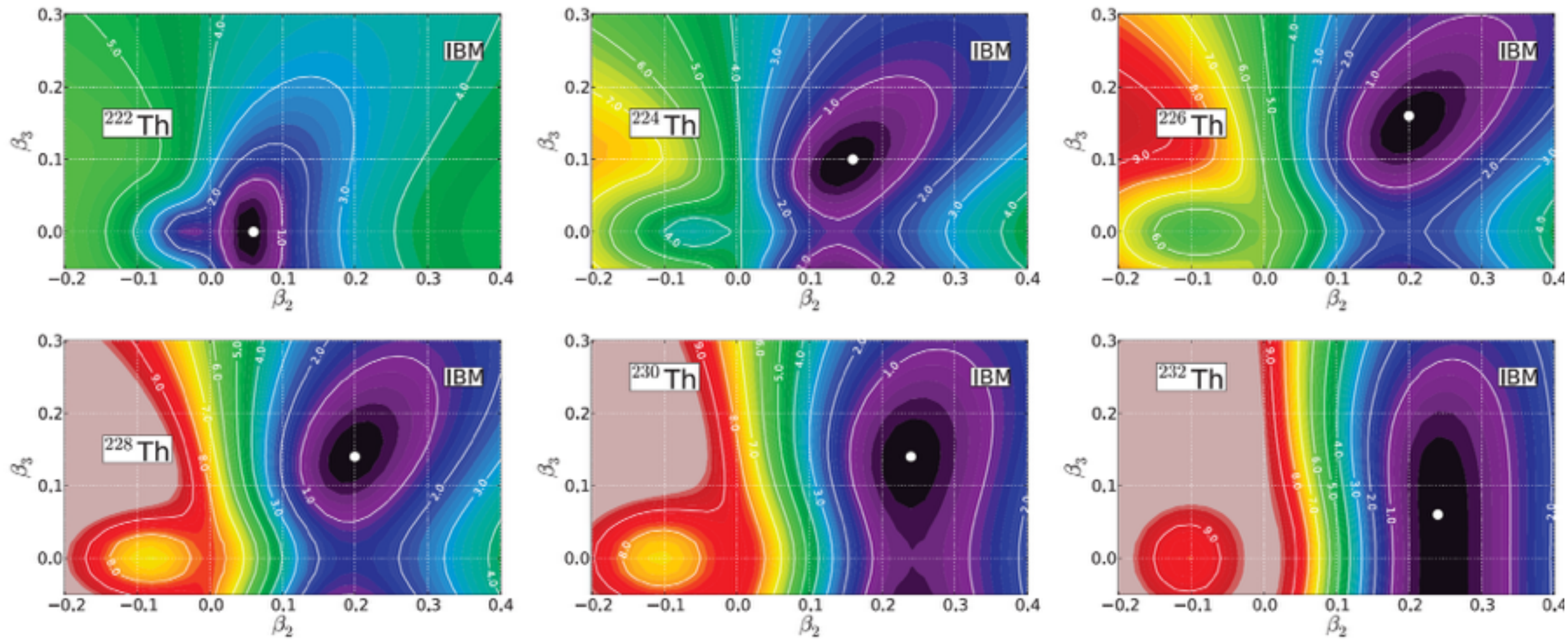

^{222}Th
^{224}Th
^{226}Th
^{228}Th
^{230}Th
^{232}Th
IBM
β_2
β_3

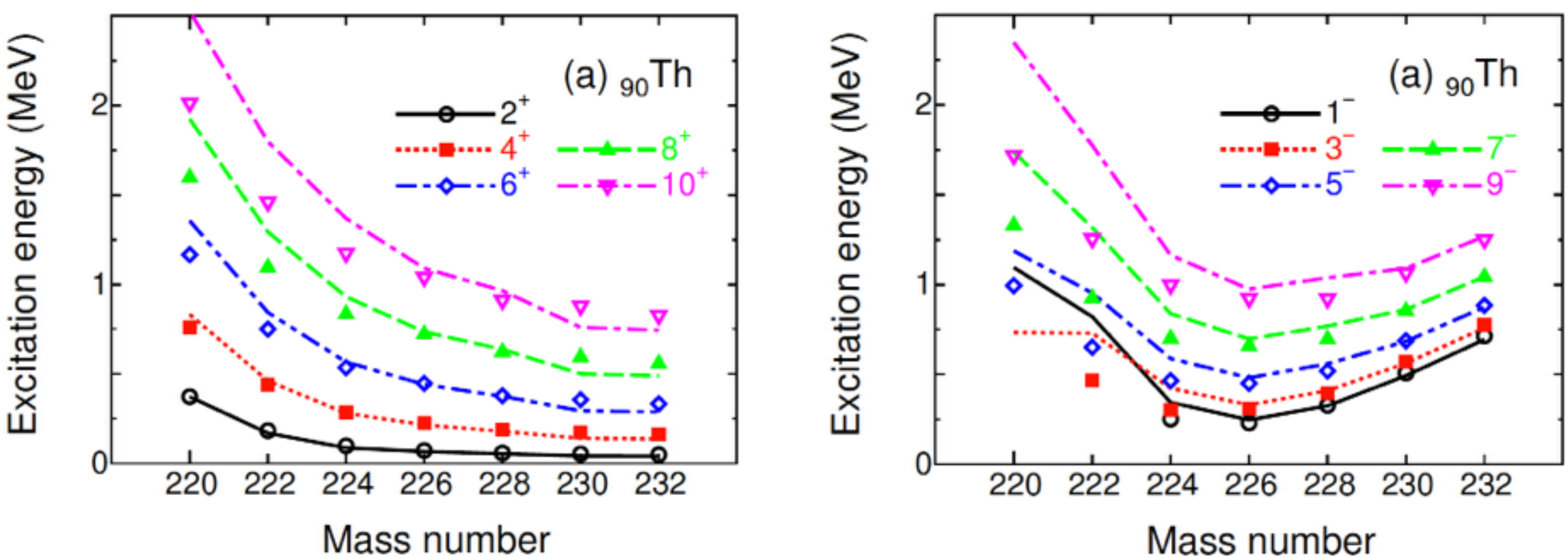

(a) $_{90}$Th
2^+
4^+
6^+
8^+
10^+
1^-
3^-
5^-
7^-
9^-
Excitation energy (MeV)
Mass number

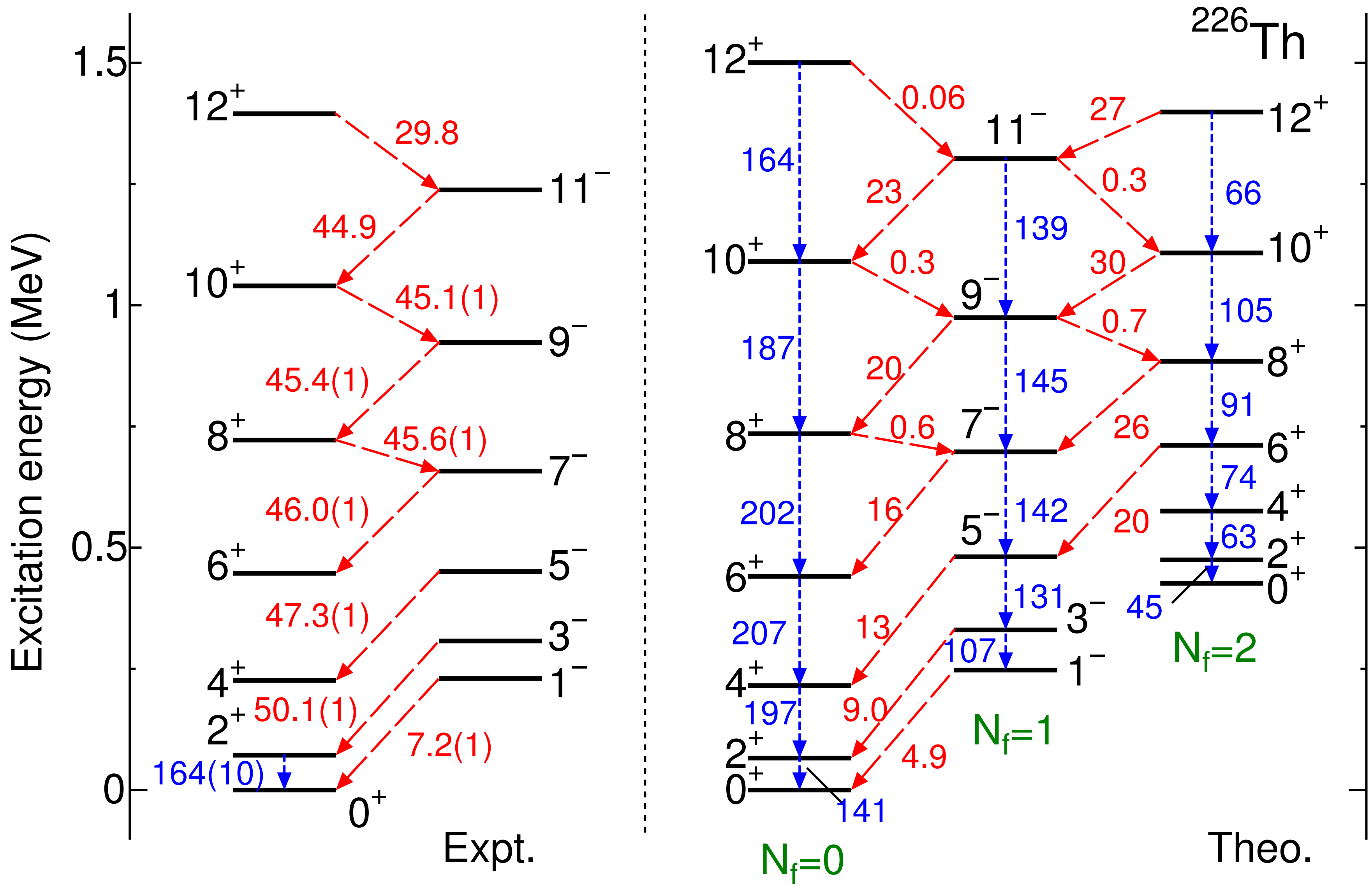

Excitation energy (MeV)
1.5
1
0.5
0
12+
10+
8+
6+
4+
2+
0+
11−
9−
7−
5−
3−
1−
29.8
44.9
45.1(1)
45.4(1)
45.6(1)
46.0(1)
47.3(1)
50.1(1)
7.2(1)
164(10)
Expt.
226Th
0.06
27
164
23
0.3
66
139
0.3
30
187
20
0.7
105
145
0.6
26
91
202
16
142
74
20
63
45
207
13
131
107
197
9.0
4.9
141
Nf=0
Nf=1
Nf=2
Theo.

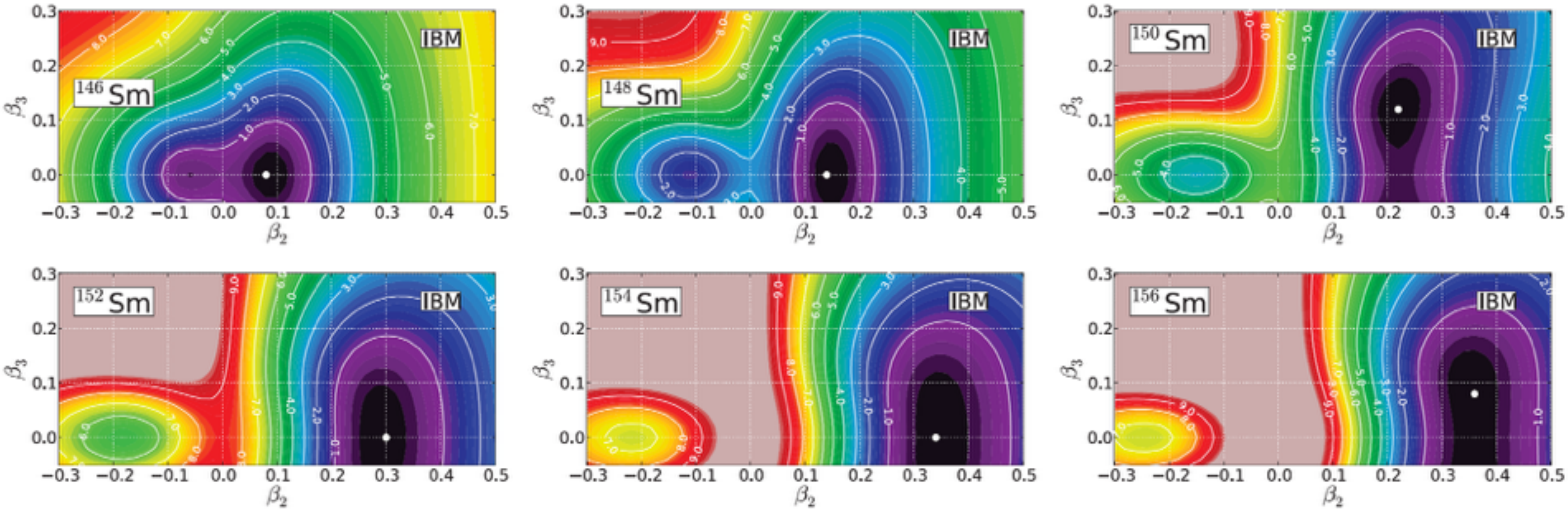

POSITIVE PARITY

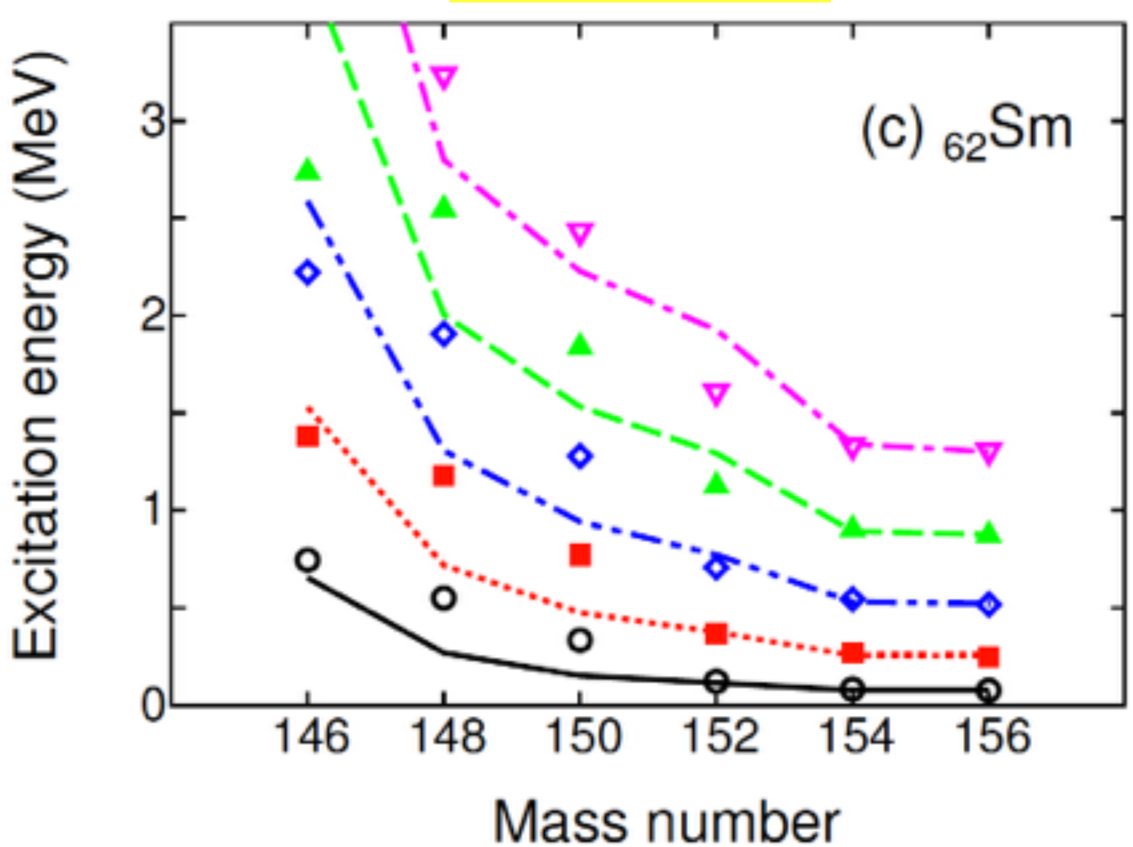

NEGATIVE PARITY

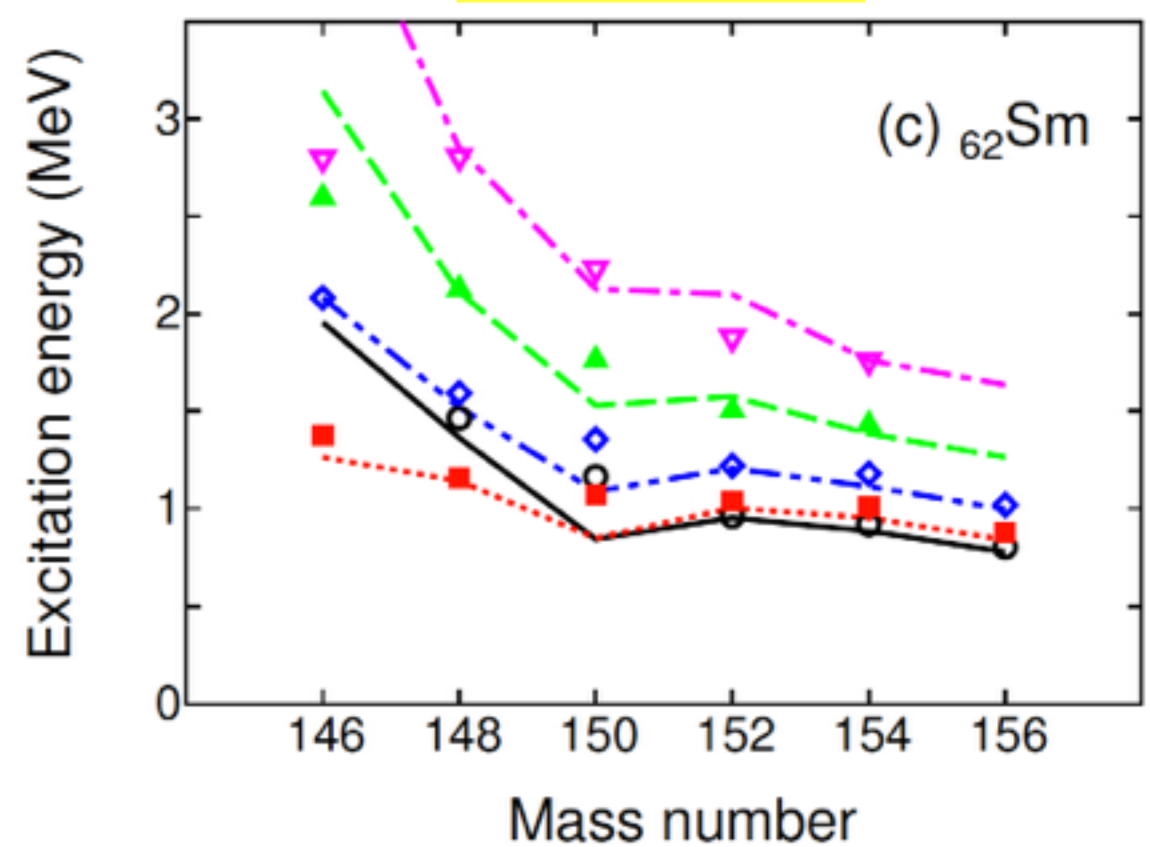

Localization and clustering in the nuclear Fermi liquid

^{20}Ne

Equilibrium properties calculated using two different density functionals:

	Skyrme SLy4	Rel. DD-ME2	EXP
Binding energy	157.2 MeV	156.4 MeV	160.6 MeV
Charge radius	3.04 fm	2.98 fm	3.0 fm
Matter radius	2.92 fm	2.86 fm	2.85 fm
Deformation	β	β	

^{20}Ne: intrinsic equilibrium density distributions

Skyrme Ly4

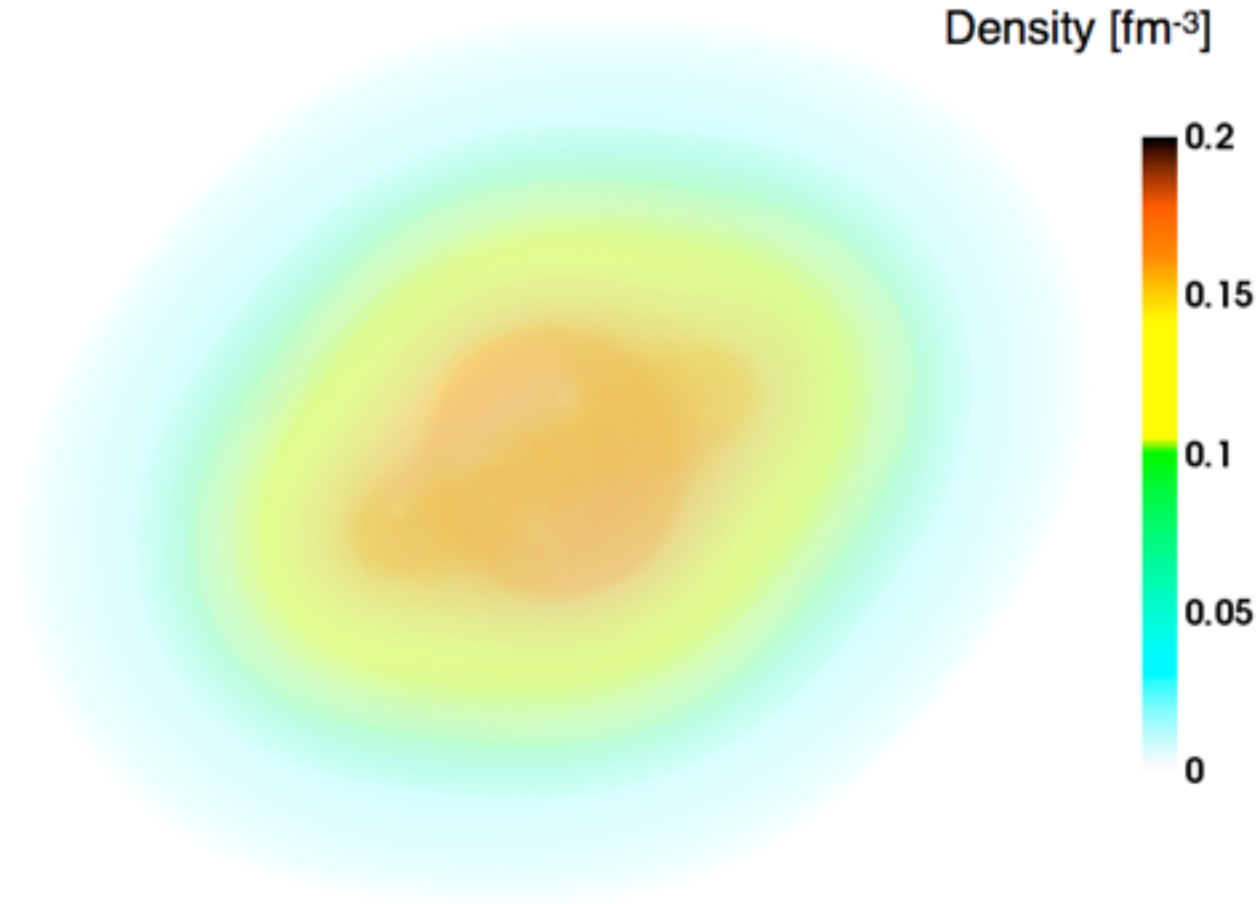

DD-ME2

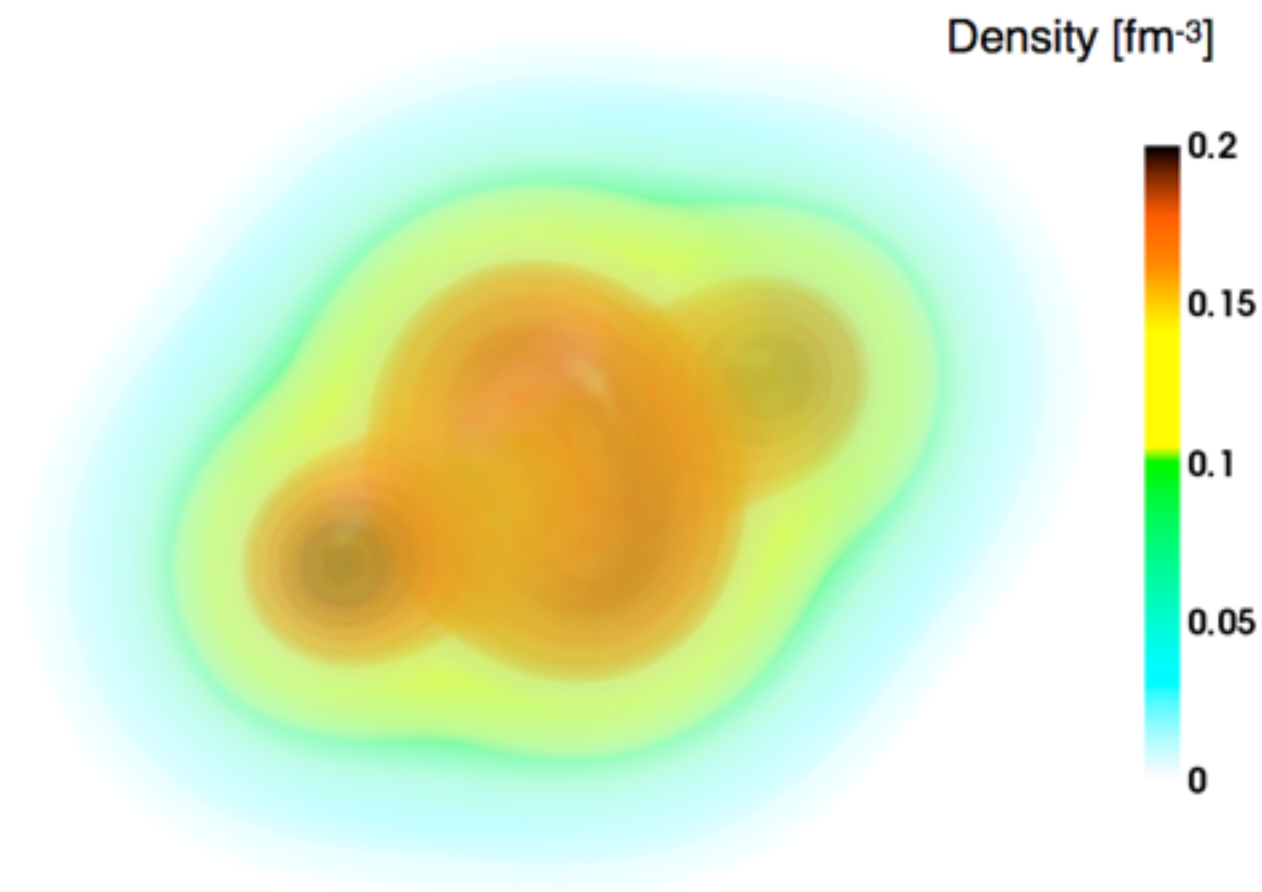

^{28}Si: intrinsic equilibrium density distributions

Skyrme Ly4

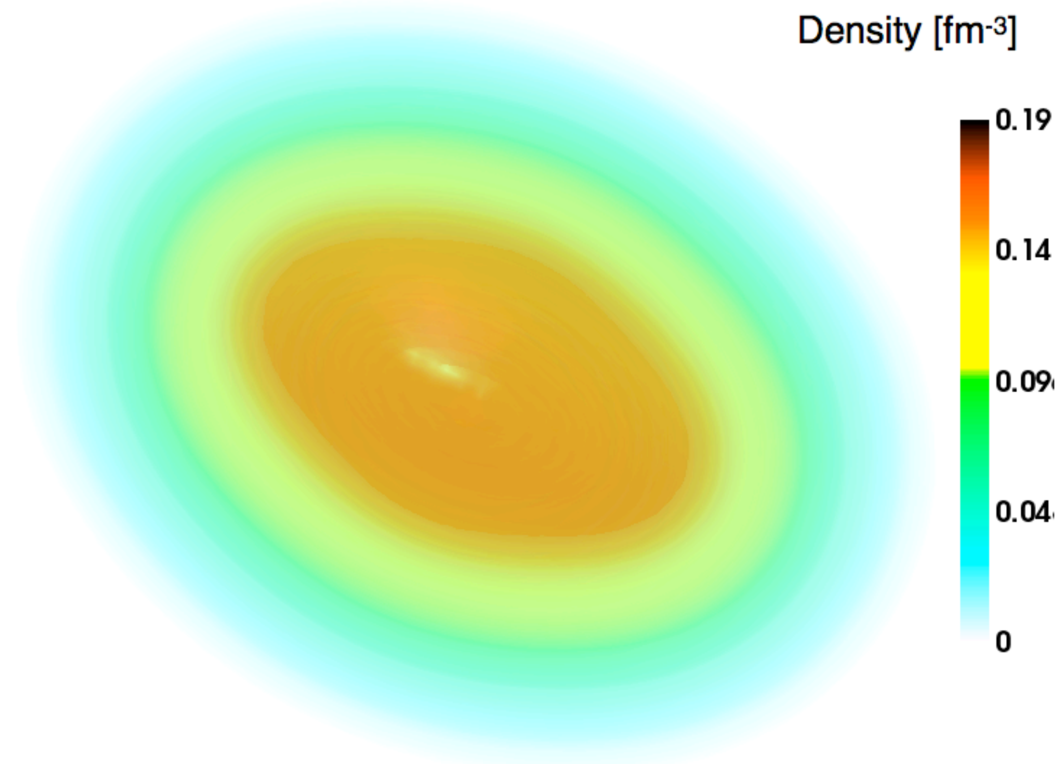

DD-ME2

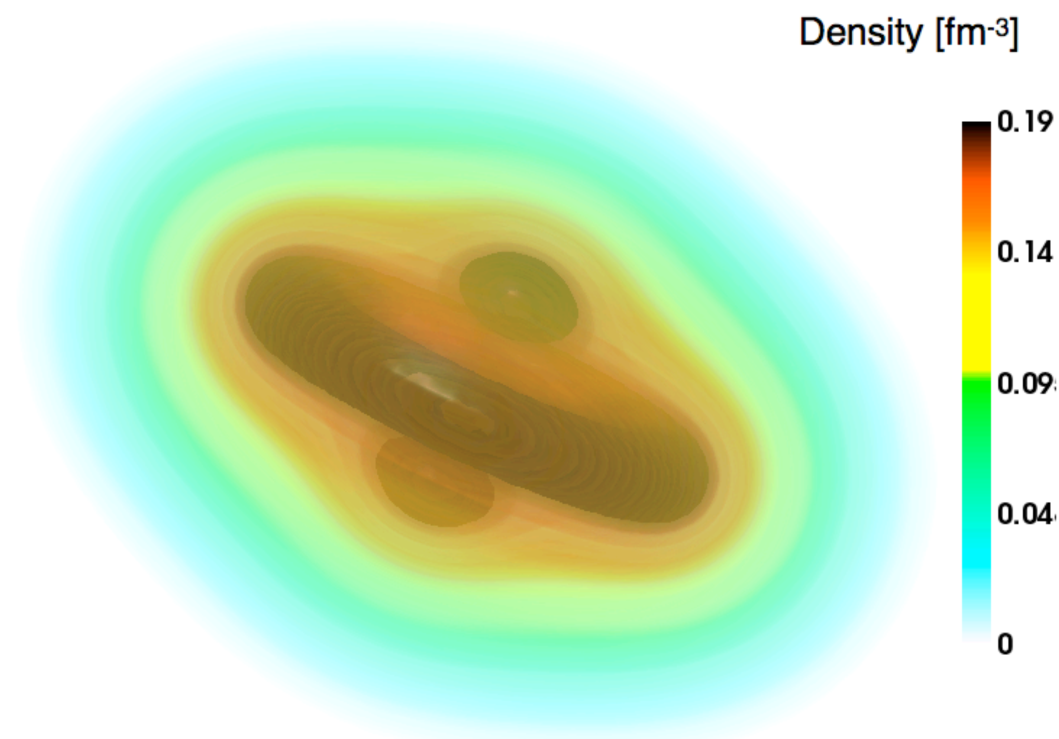

^{20}Ne: intrinsic equilibrium density distributions

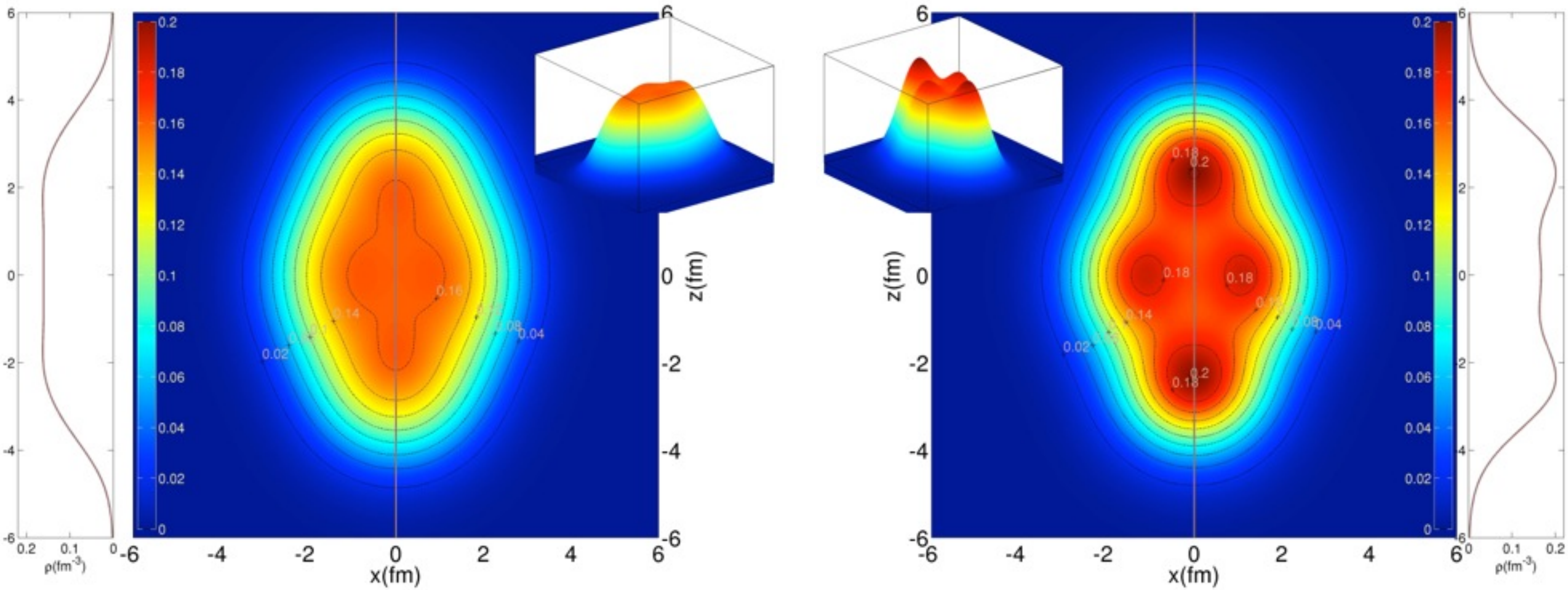

How atomic nuclei cluster

RESEARCH LETTER

J.-P. Ebran[1], E. Khan[2], T. Nikšić[3] & D. Vretenar[3]

VOL 487 | NATURE | 341

Effect of the depth of the confining potential:

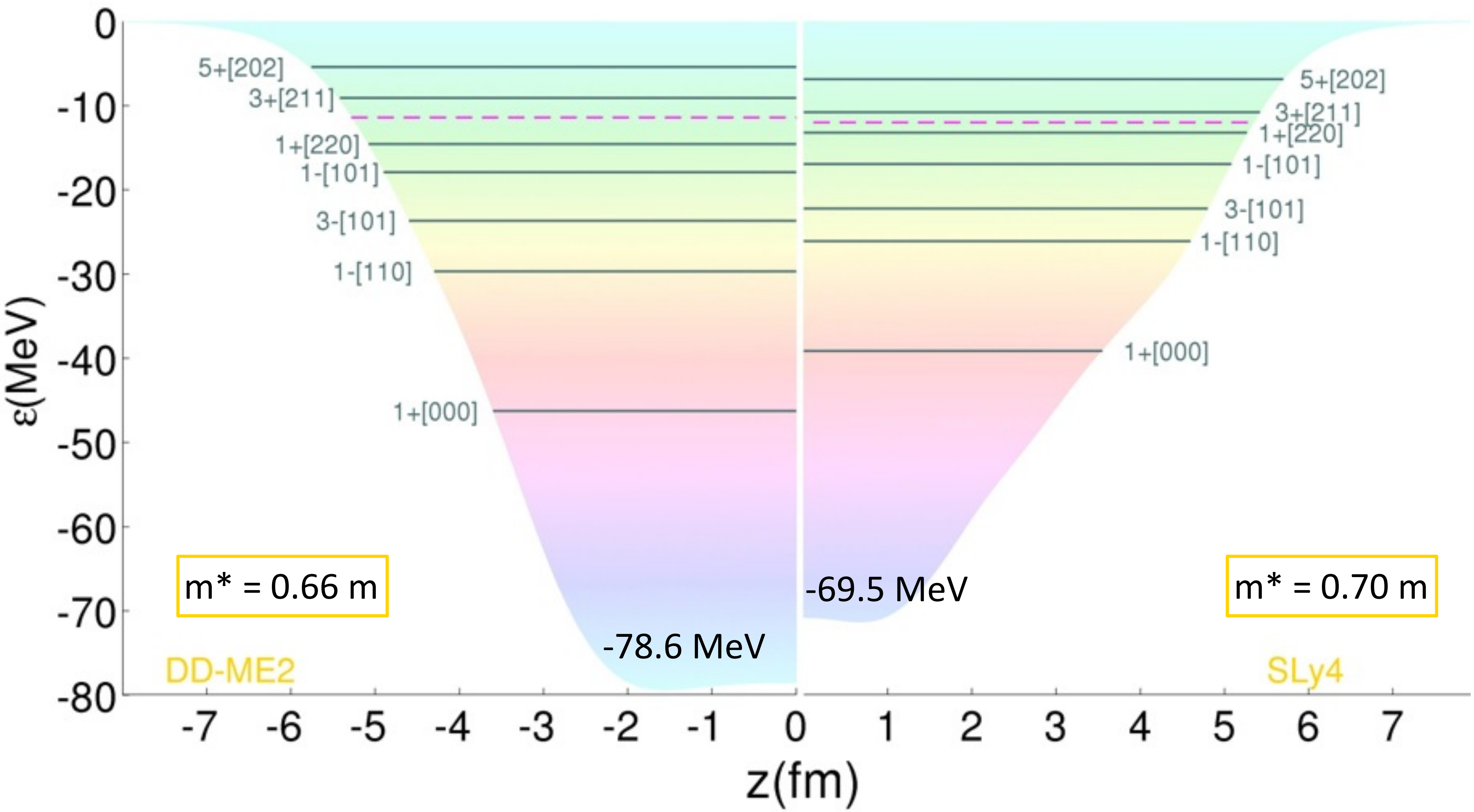

^{20}Ne – single-neutron Nilsson levels at equilibrium deformation

Effect of the depth of the confining potential:

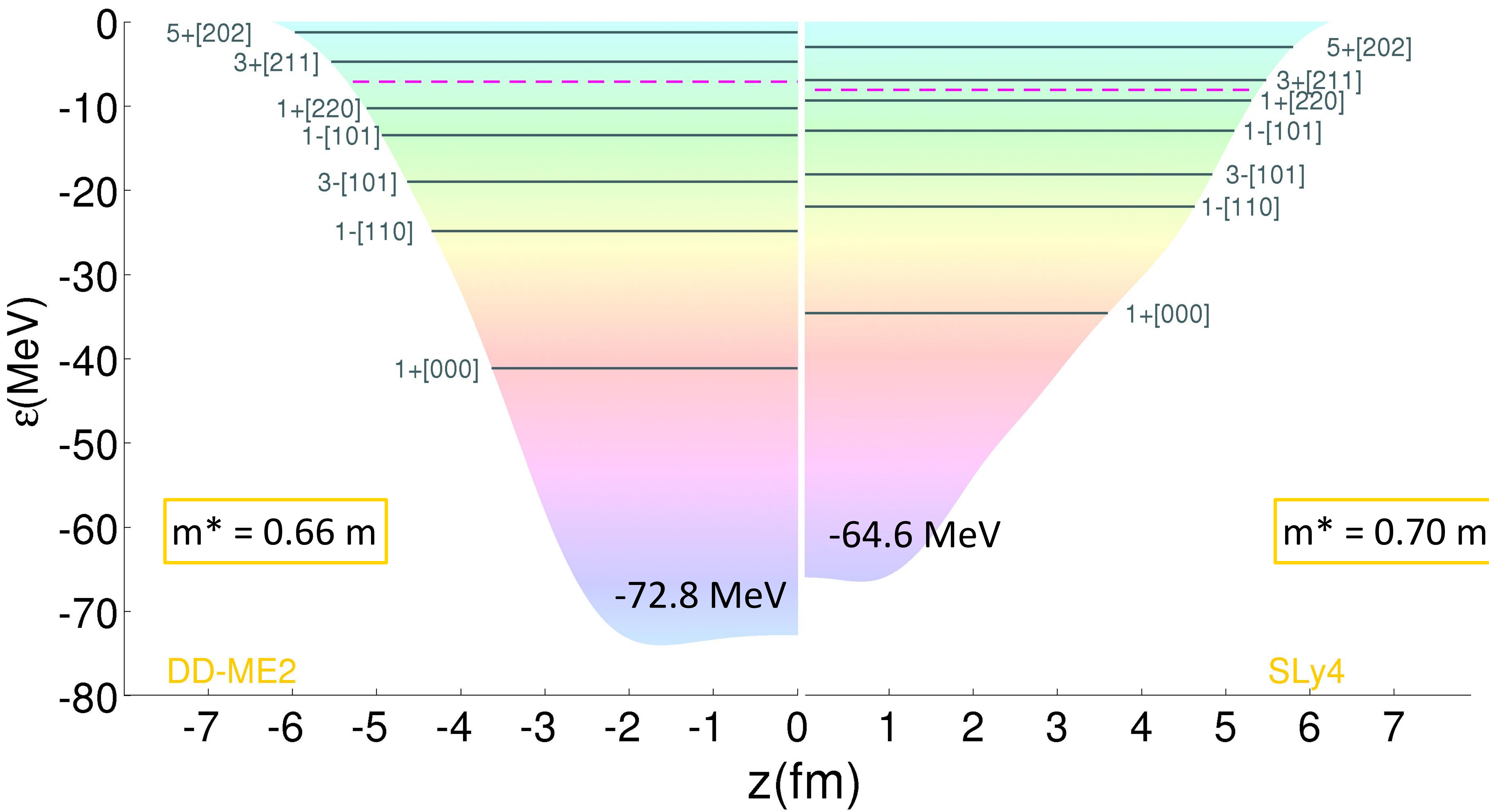

^{20}Ne – single-proton Nilsson levels at equilibrium deformation

Partial nucleon density distributions: highest occupied level 1/2$^+$[220]

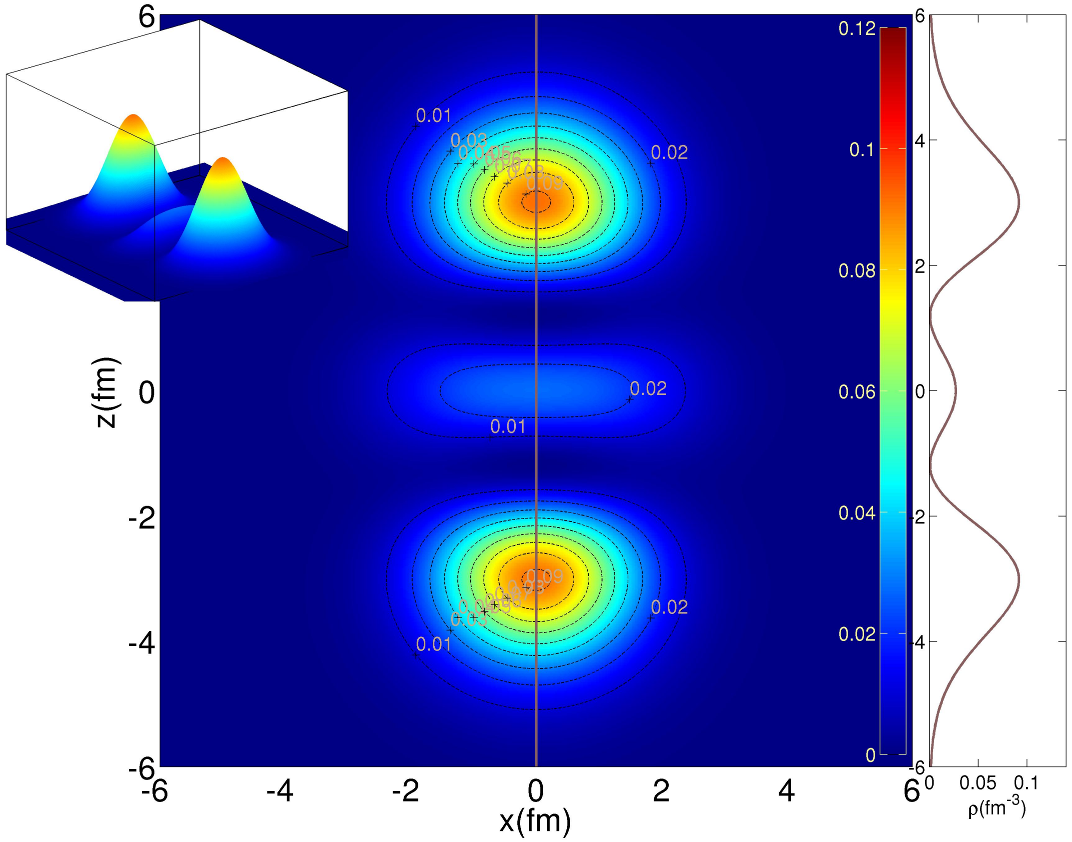

DD-ME2

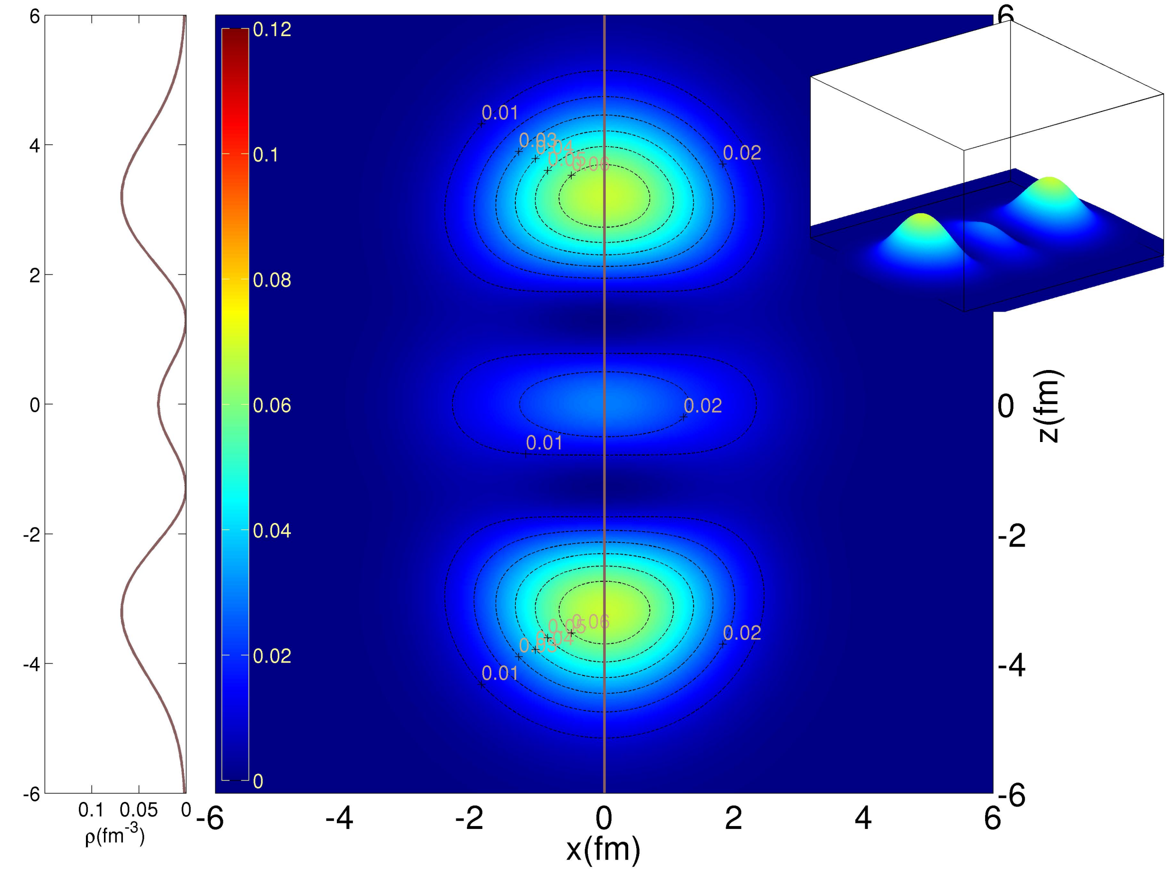

Skyrme Ly4

Spherical harmonic oscillator potentials of different depths but with the same radius → 3 fm.

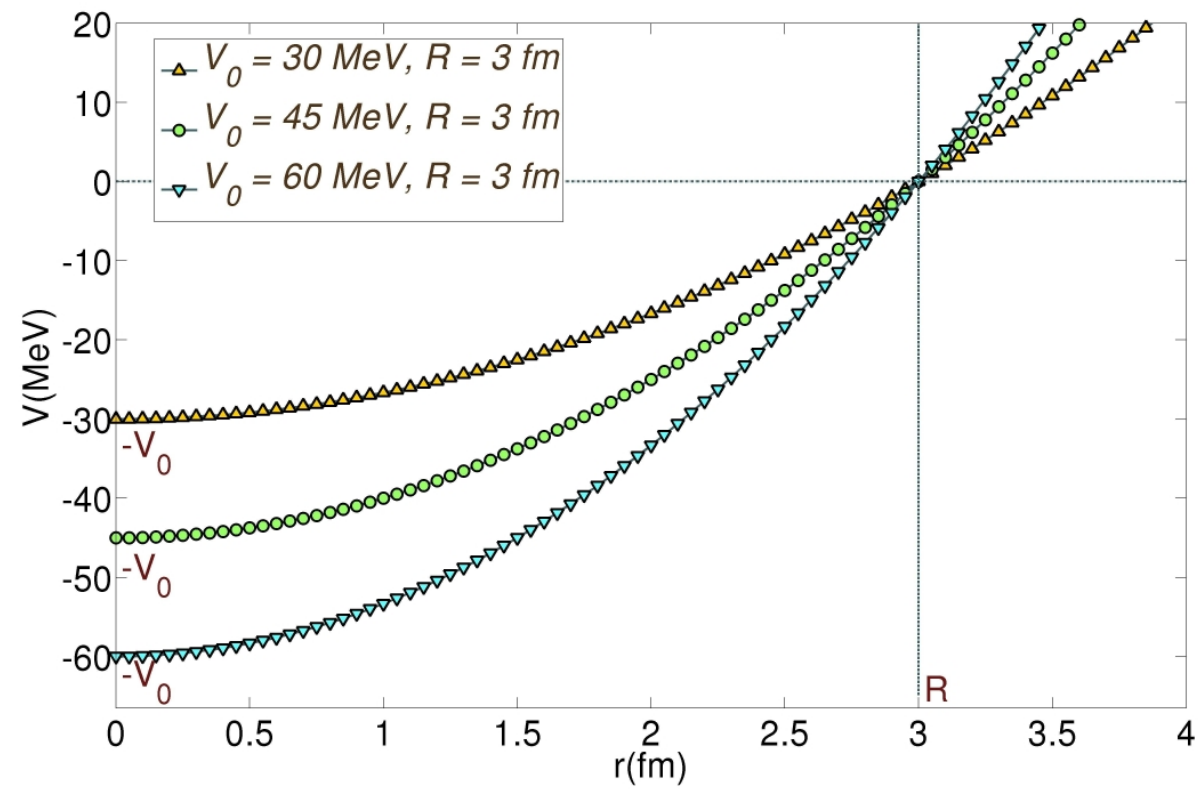

Radial wave functions of the corresponding first p-state.

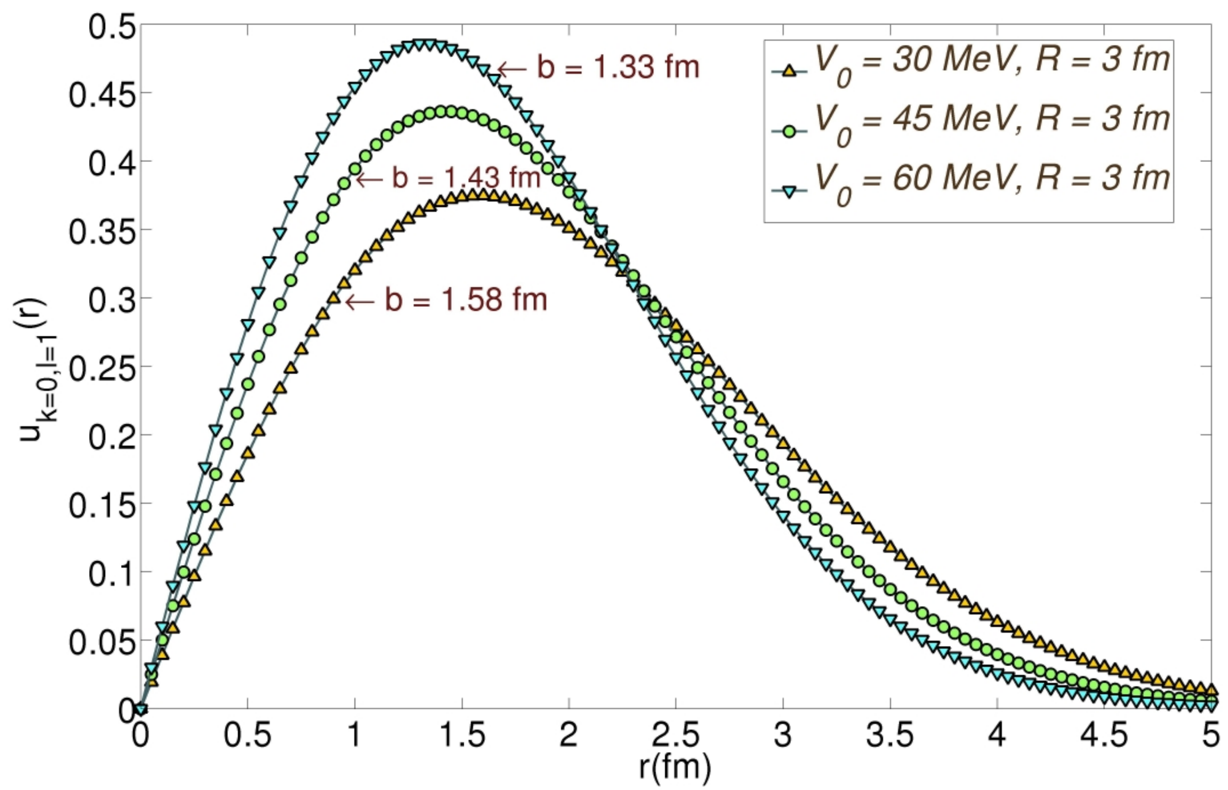

Transition from a crystalline to a quantum liquid phase:

b ➞ dispersion of the single-fermion wave function
r_0 ➞ typical inter-nucleon distance

$$\alpha = b/r_0$$

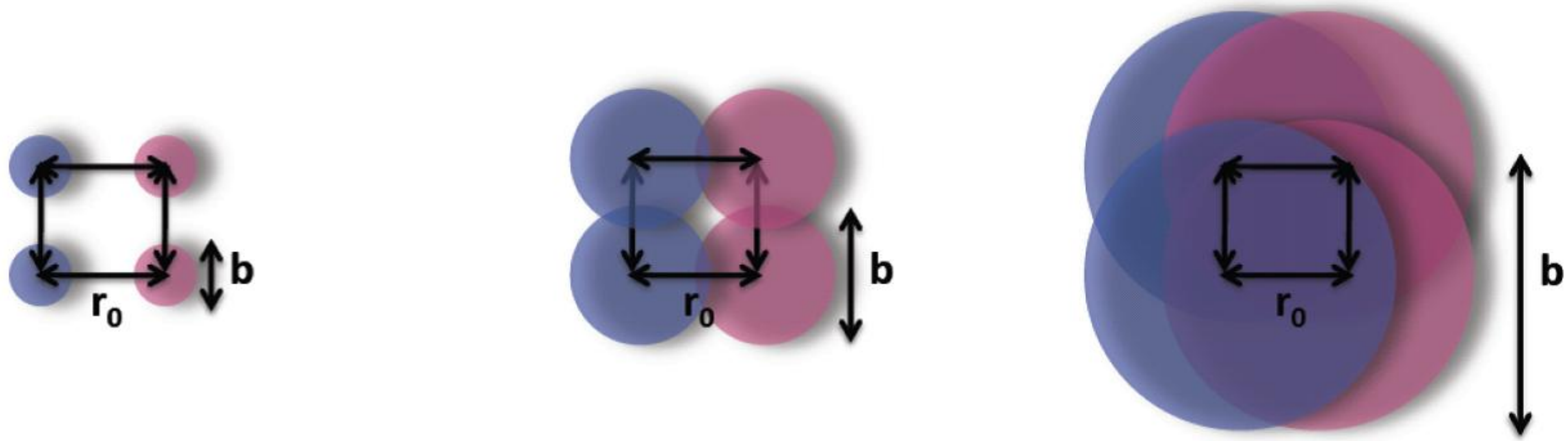

Crystal
$\alpha < 1$

Molecule
$\alpha \sim 1$

Quantum
liquid
$\alpha > 1$

EBRAN, KHAN, NIKŠIĆ, AND VRETENAR PHYSICAL REVIEW C **87**, 044307 (2013)

Role of nuclear saturation ⇒ spontaneous α-clustering at low density

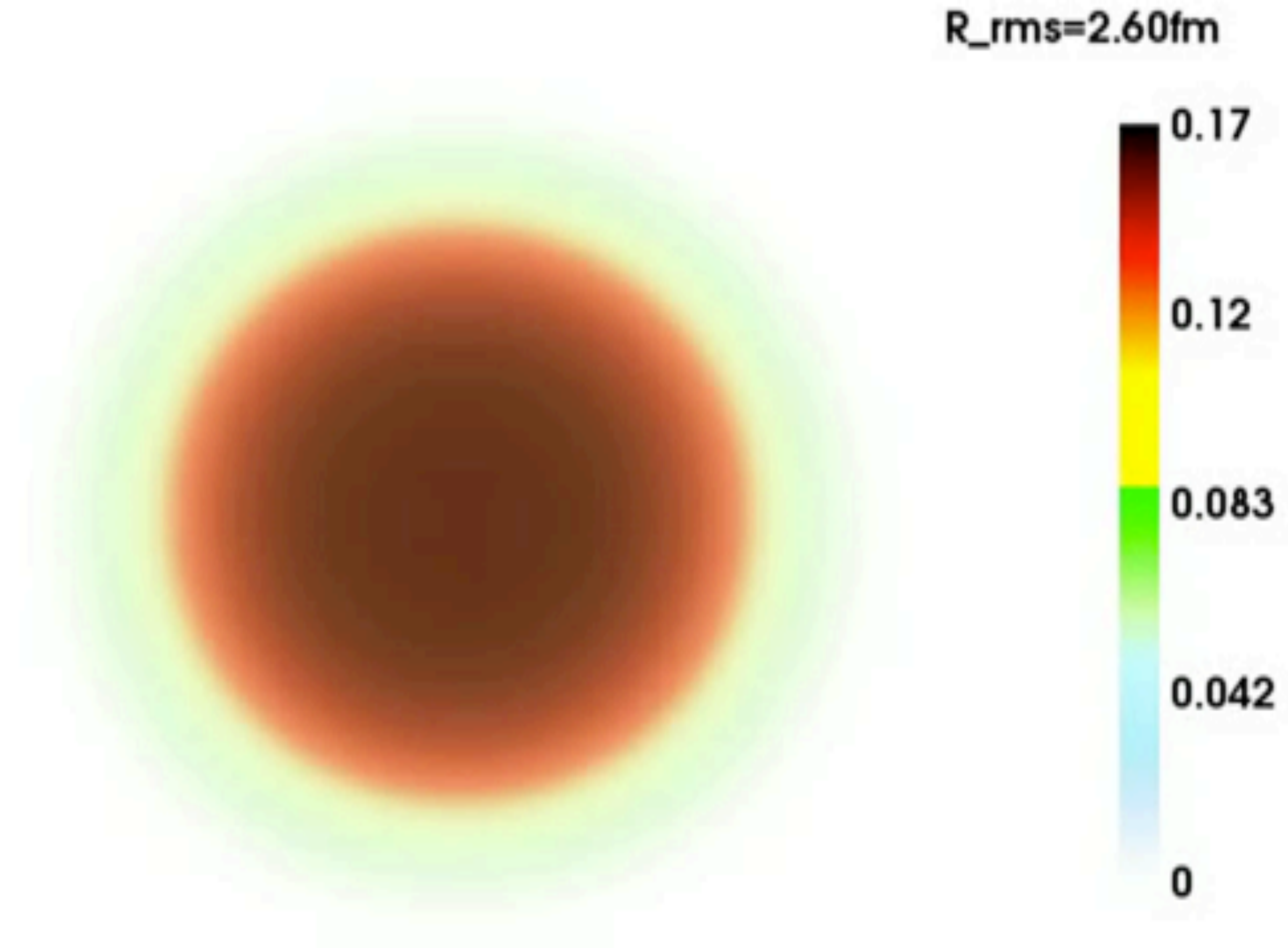

EBRAN, KHAN, NIKŠIĆ, AND VRETENAR

PHYSICAL REVIEW C **89**, 031303(R) (2014)

β-decay half-lives of neutron-rich nuclei and matter flow in the r-process

Niu, Niu, Liang, Long, Nikšić, Vretenar, Meng, Phys. Lett. B **723**, 172 (2013).

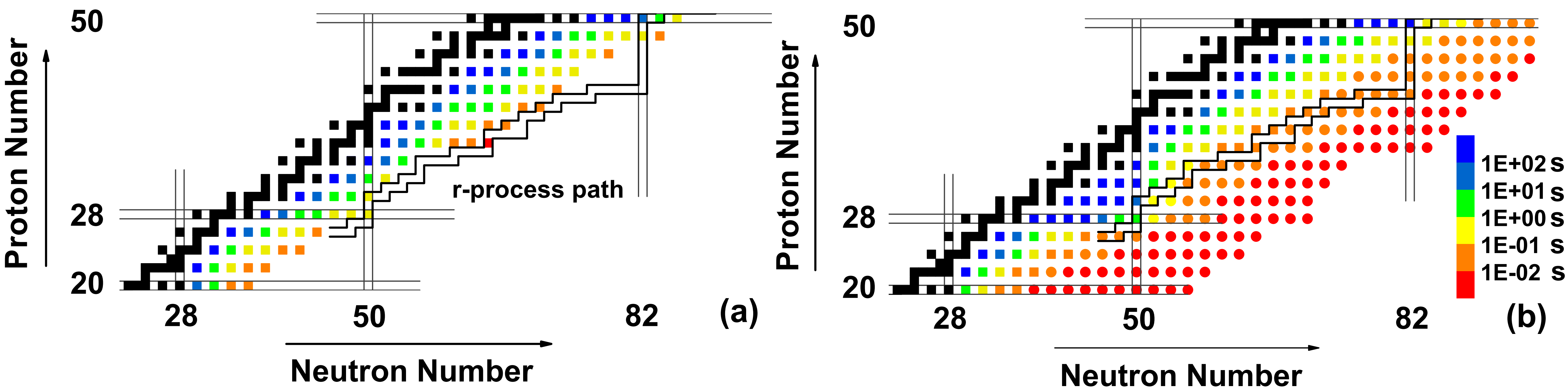

Contour maps of experimental and theoretical β-decay half-lives for the Z = 20-50 even–even nuclei.

Half-lives of r-process bottleneck nuclei near N = 82

Nucleus	Half-life (s)		
	RHFB + QRPA	FRDM + QRPA	Exp.
^{124}Mo	0.0108	0.0106	–
^{126}Ru	0.0205	0.0342	–
^{128}Pd	0.0486	0.1251	–
^{130}Cd	0.1685	1.1232	0.162 ± 0.007
^{134}Sn	0.7530	3.5410	1.050 ± 0.011

➔ impact of the predicted β-decay half-lives on r - process abundances:

The impact of nuclear β-decay half-lives on the r-matter flow. The curves correspond to calculated r-process abundances in comparison to data denoted by the points. Panels (a) - (d) correspond to neutron irradiation times τ_r = 1.5, 2.0, 2.5, and 3.0 s.

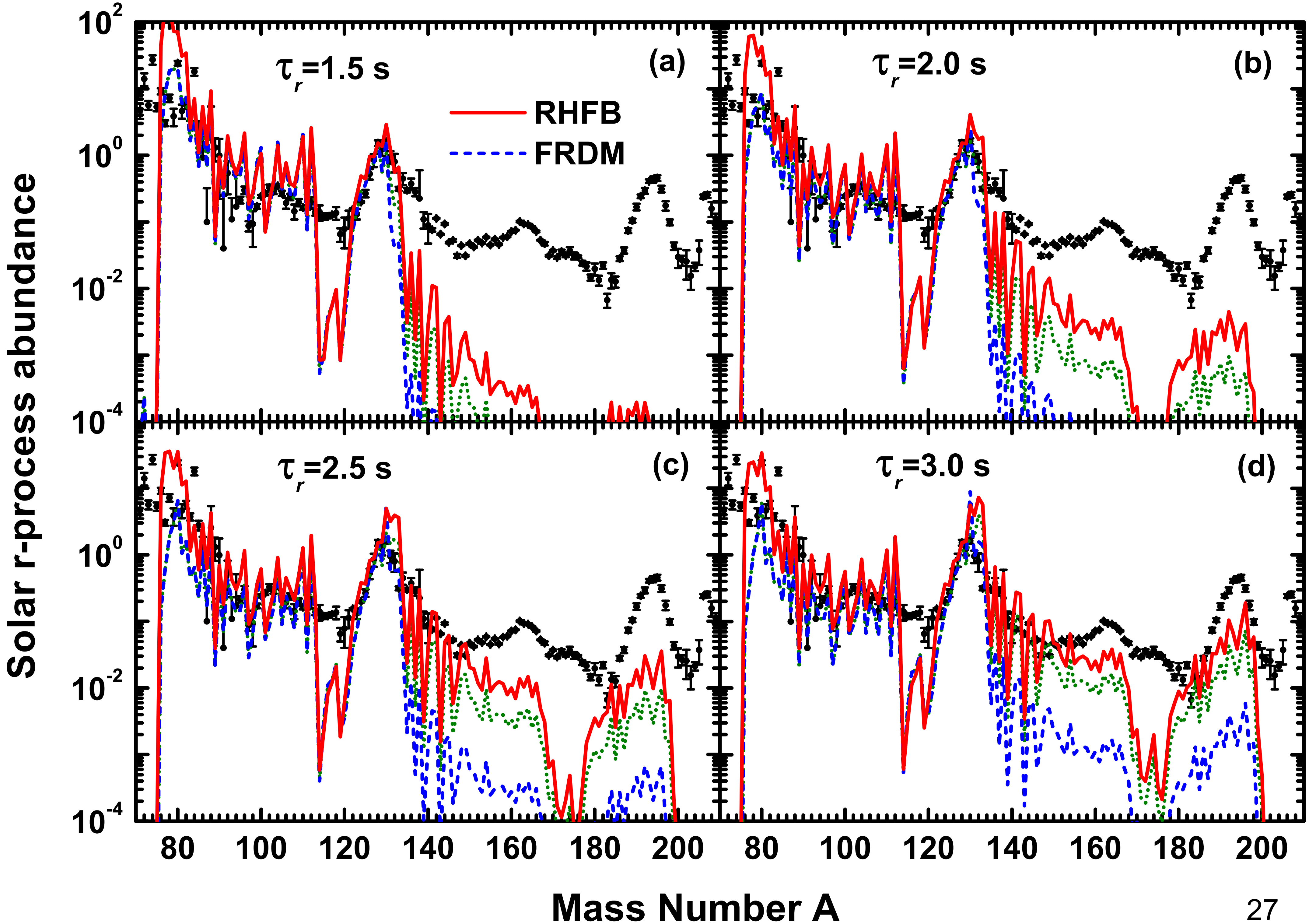

Nuclear Energy Density Functional Framework

✔ unified microscopic description of the structure of stable and nuclei far from stability, and reliable extrapolations toward the drip lines.

✔ when extended to take into account collective correlations, EDFs describe deformations, shape-coexistence and shape-phase transition phenomena associated with shell evolution.

✔ Time-dependent NDFT → fully self-consistent (Q)RPA analysis of giant resonances, low-energy multipole response in weakly-bound nuclei, astro-physical applications.